

# Ioni energetici nella sintesi e caratterizzazione di materiali e dispositivi avanzati

Valentino Rigato

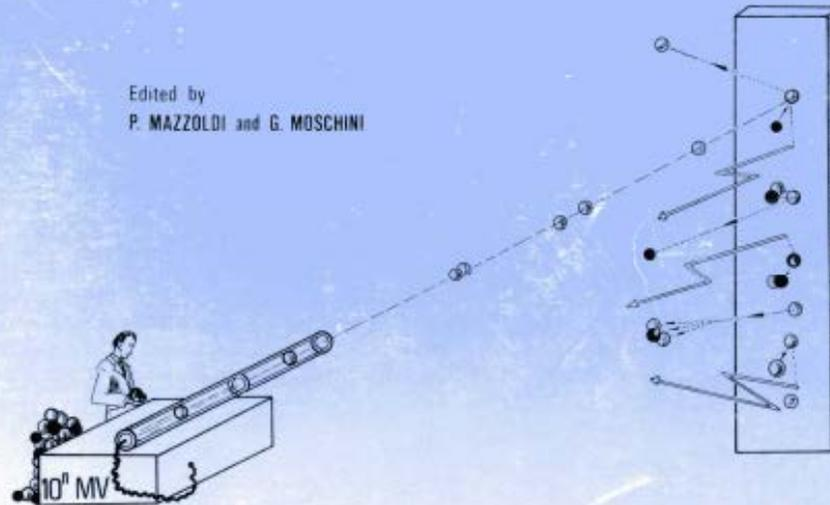
LNL - 18 novembre 2021 - PID

Proceedings

*International Symposium*  
on

THREE-DAY IN DEPTH-REVIEW ON THE NUCLEAR ACCELERATOR  
IMPACT IN THE INTERDISCIPLINARY FIELD

Edited by  
P. MAZZOLDI and G. MOSCHINI



Laboratori Nazionali di Legnaro (Padova), Italy

May 30<sup>th</sup> - June 1<sup>st</sup>, 1984

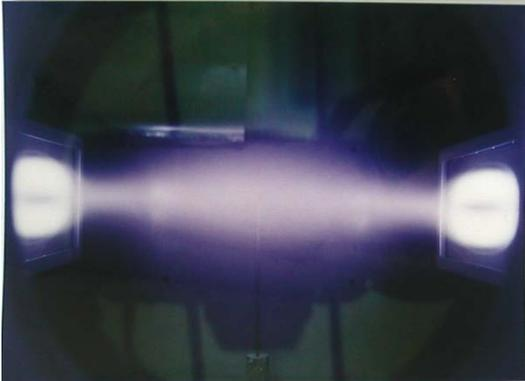
# ENERGIA E CAMPI DI APPLICAZIONE DI FASCI IONICI

IONI PESANTI  
Ar, Xe, Kr, Metalli

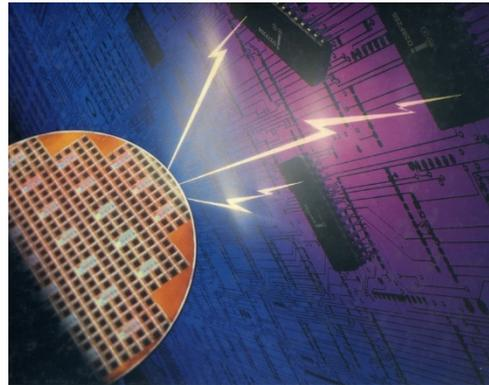
IONI PESANTI  
C, N - B, P, As....

IONI LEGGERI  
Protoni, He, Li

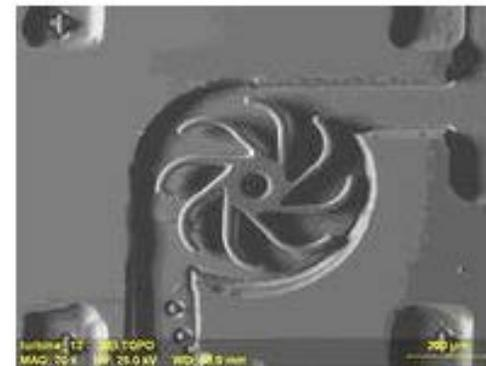
1eV                      1000eV                      1keV                      500keV                      1MeV                      10MeV



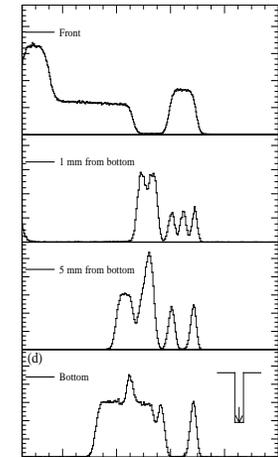
Sintesi di nuovi materiali  
Trattamenti superficiali  
Plasmi a bassa pressione



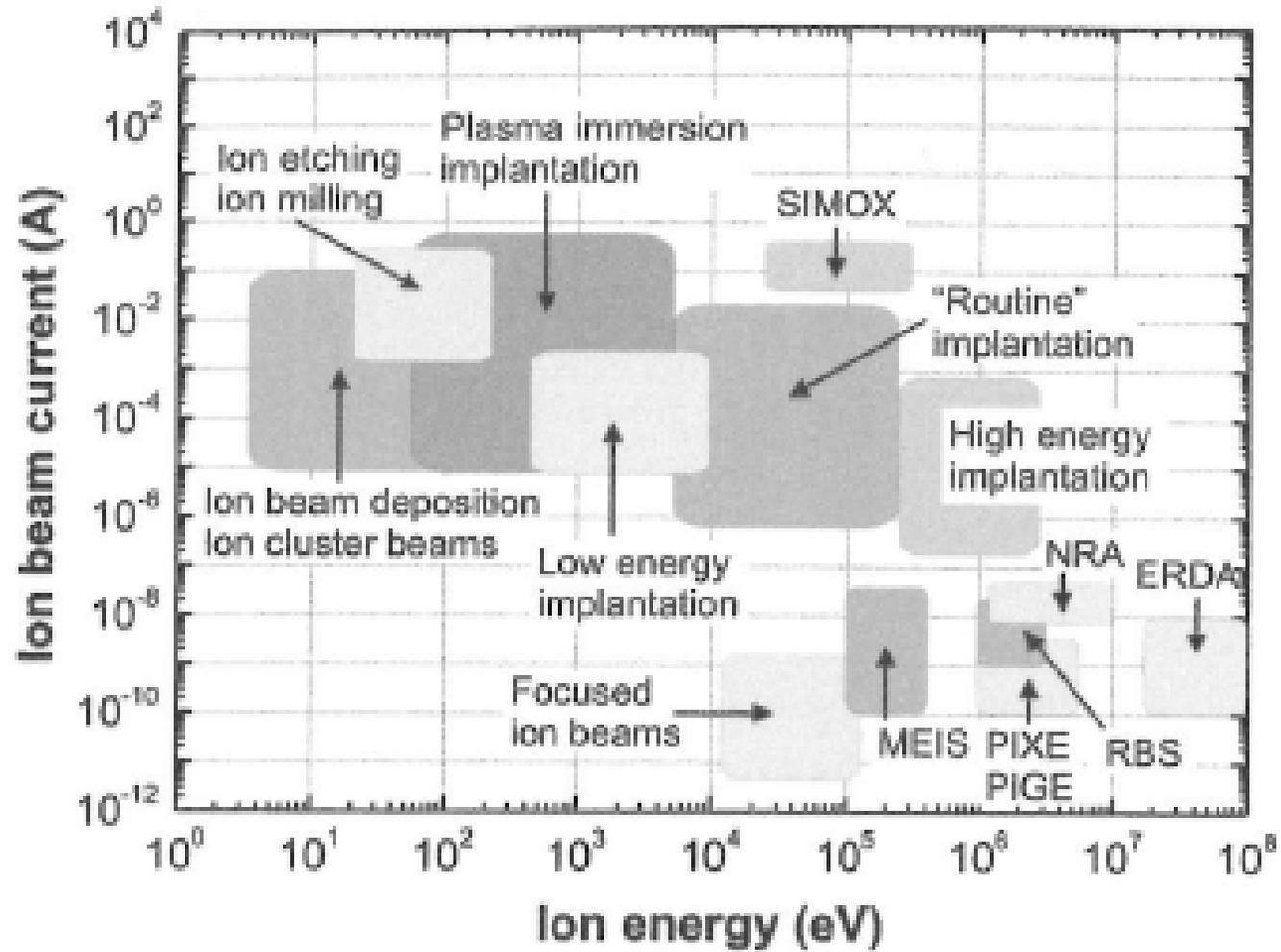
Impiantazione ionica  
Drogaggio di semiconduttori



Microanalisi di materiali (RBS, PIXE, PIGE, ERD, NRA)  
Microfabbricazione



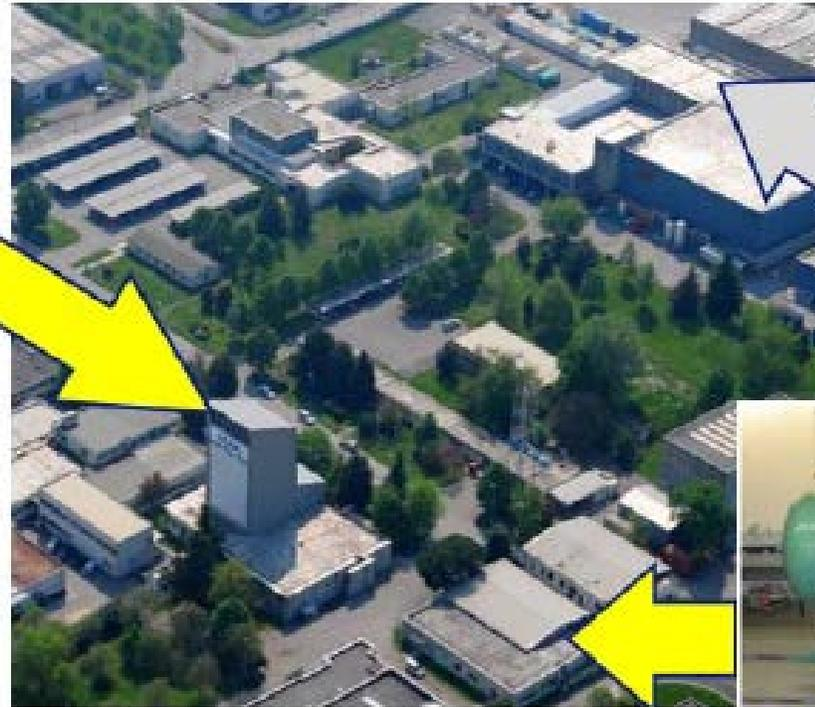
Ion current – energy map of ion beam techniques for material processing and analysis



# Acceleratori usati in esperimenti di fisica interdisciplinare presso i Laboratori Nazionali di Legnaro



**CN: 1-6 MV**  
(Van de Graaff)



TANDEM-  
XTU-ALPI

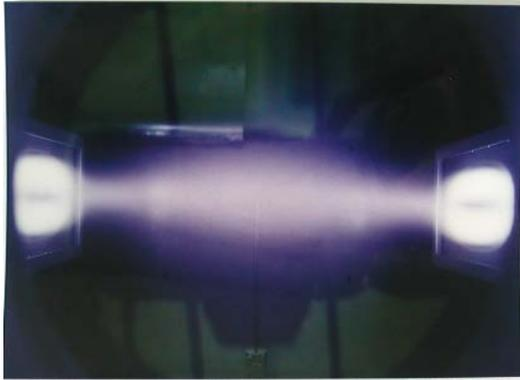


**AN2000: 0.2-2.2MV**  
(Van de Graaff)

200keV-6MeV

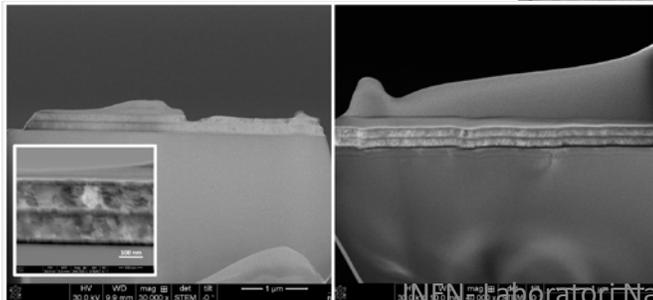
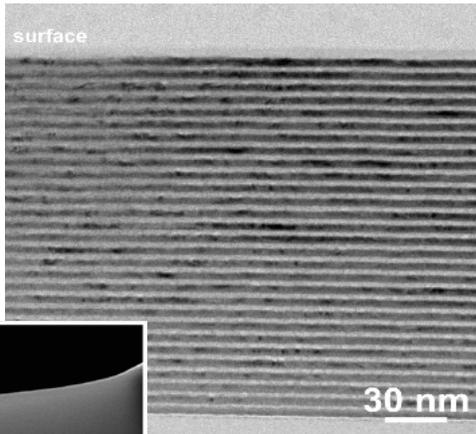
# LABORATORIO DI SINTESI E CARATTERIZZAZIONE DI MATERIALI AVANZATI

## Synthesis and Process Development



- Plasma Sputtering Deposition
- Plasma Diagnostics
- Ion-solid interaction

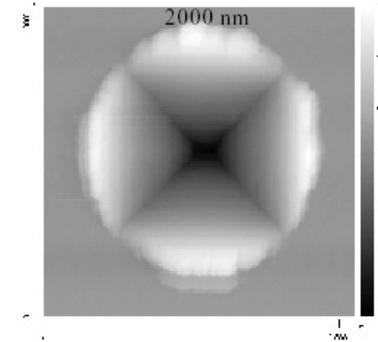
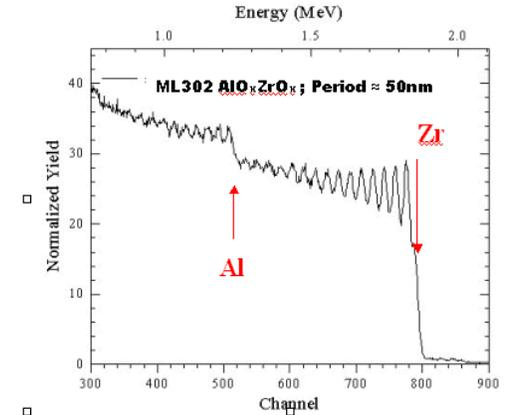
- Low Friction, High Hardness Nanoscaled Materials and Multilayers
- Insulating Oxides
- High Performance Plastics



## Characterization of Physical Properties

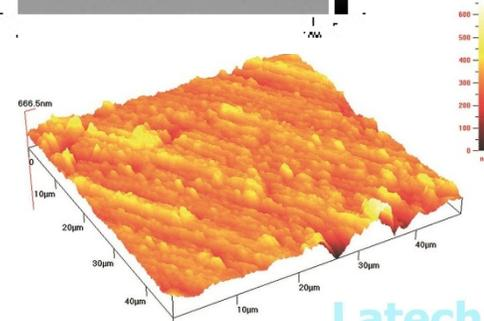
### Composition

- Ion Beam Analysis (RBS, NRA, ERDA, PIXE)
- Microbeam (Micro-PIXE 2-D trace element analysis)



### Morphology, Mechanical prop.

- Nano Hardness, Elastic modulus
- Adhesion (Micro-Scratch)
- Intrinsic Stress
- Atomic Force Microscopy & SEM



Latech

IL PLASMA COME SORGENTE DI IONI

# PLASMI (ESEMPI)

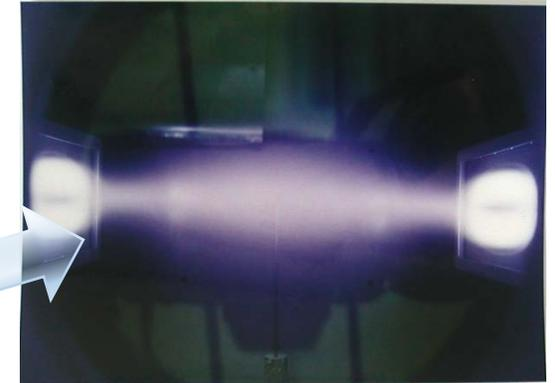
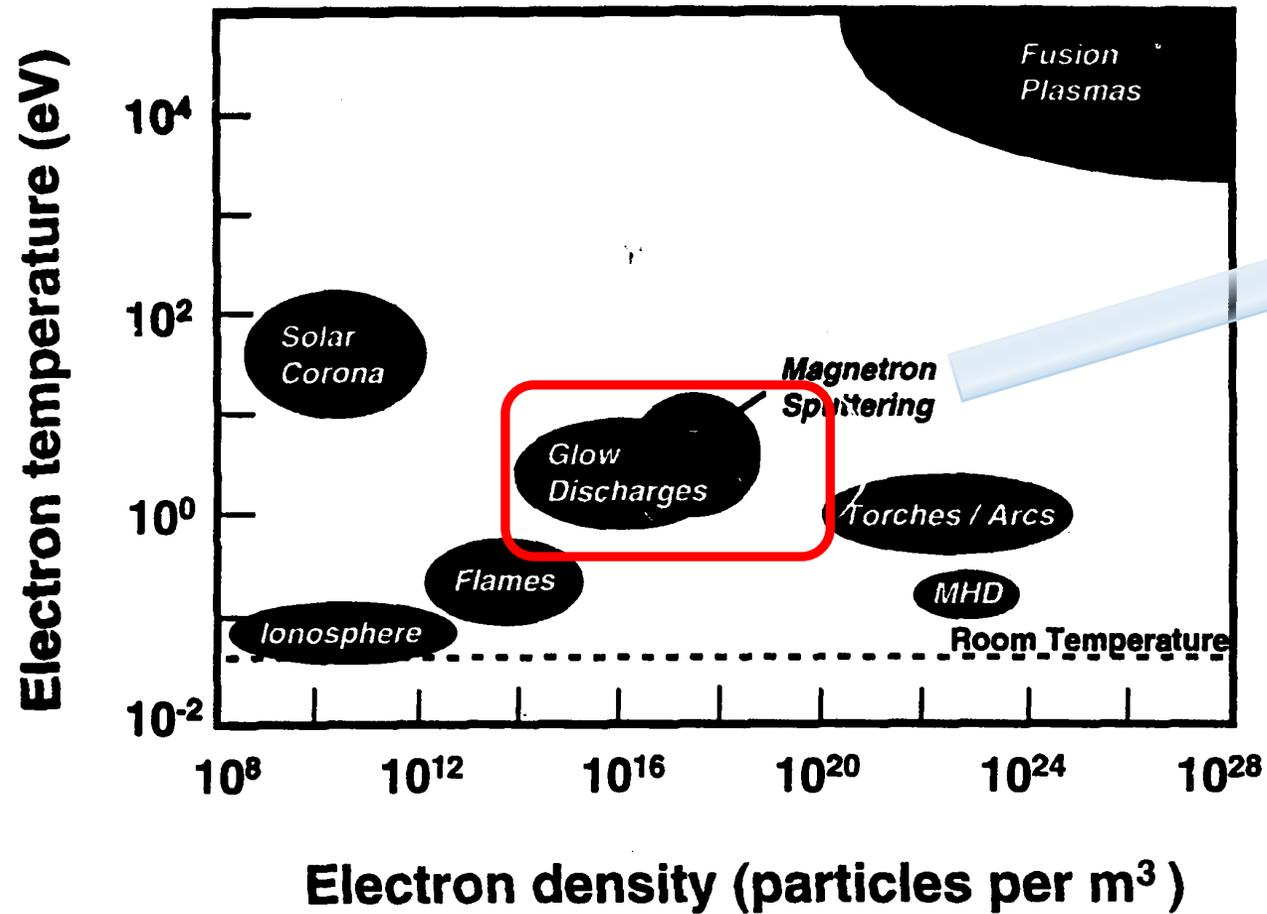
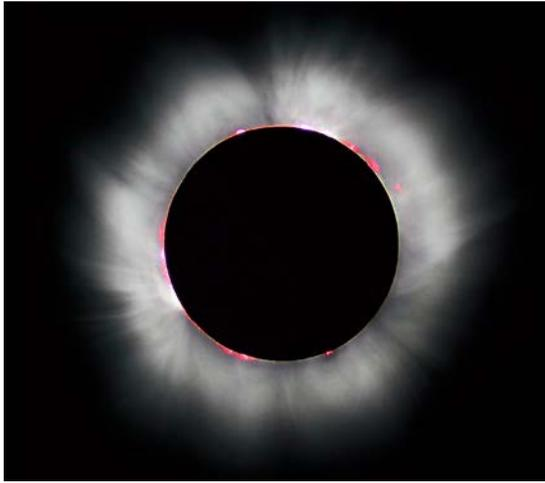


Figure 1. Classification of plasmas as a function of electron temperature and density. A convenient unit of temperature is the electron volt (eV) where 1 eV equals 11,600 K through the Boltzmann constant.

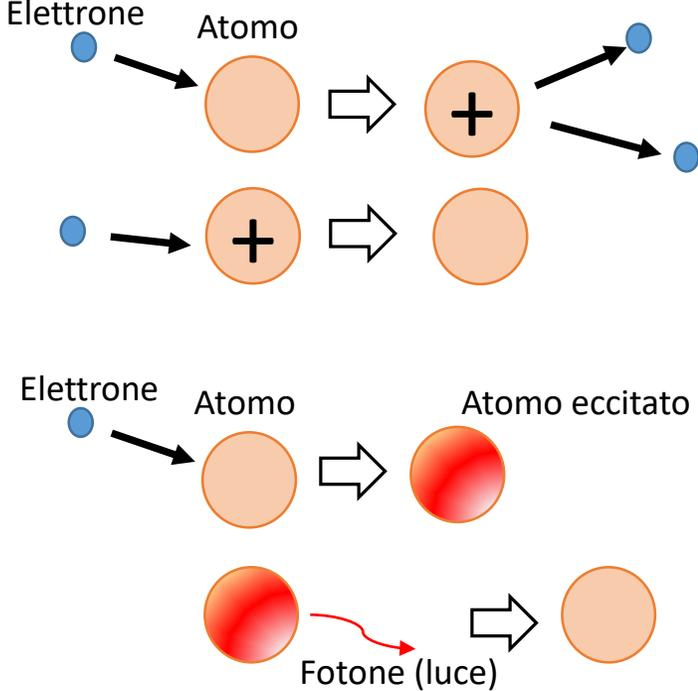
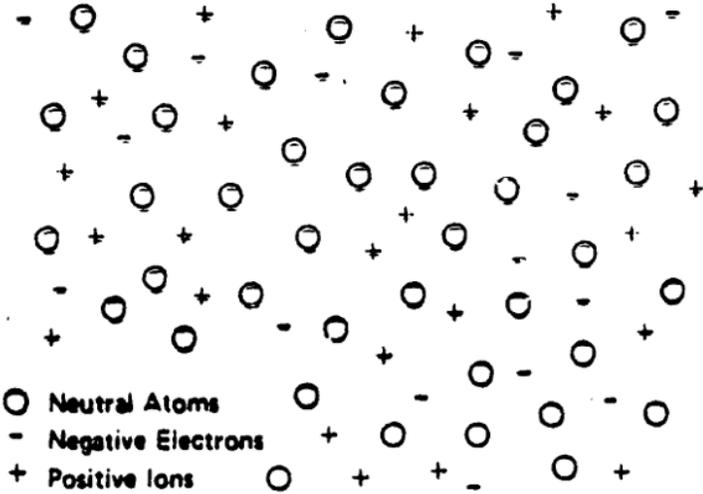
PLASMA = GLOW DISCHARGE = IONIZED GAS  
PLASMA IS OUR EXTENDED SOURCE OF IONS

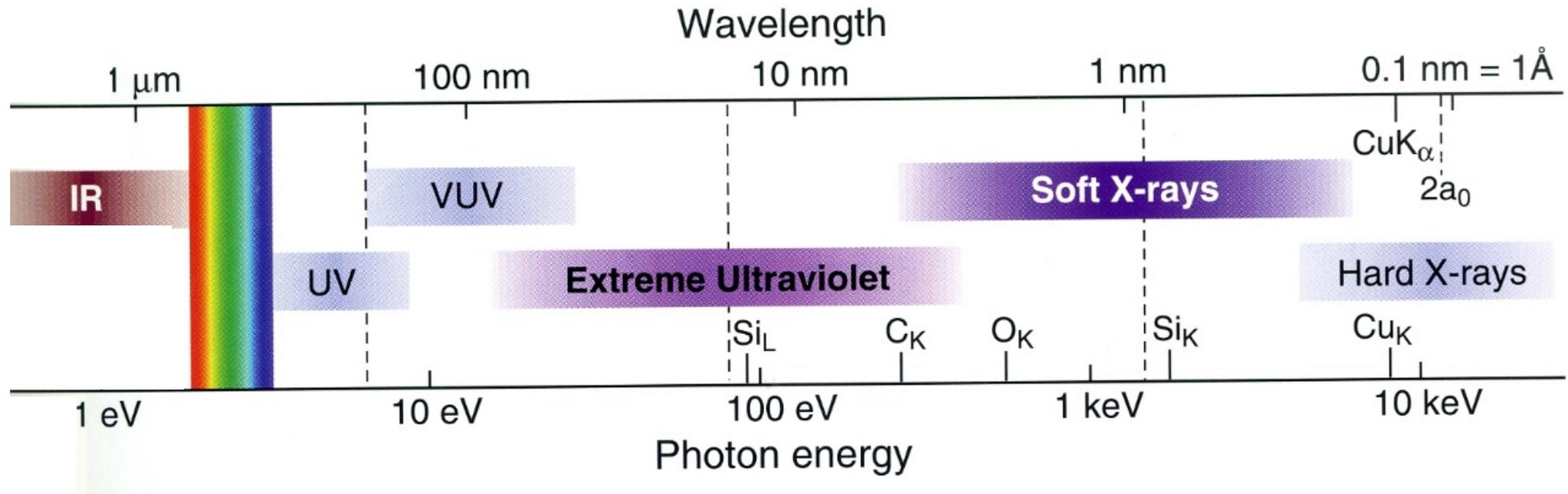
LOW PRESSURE PLASMA: a plasma derived by a low pressure gas  
Typical gas pressures for plasma sputtering:  $10^{-4}$  to  $10^{-1}$  mBar

Simple picture:

- Electron gas in thermal equilibrium
- Ion Gas in thermal equilibrium
- Neutral gas (obviously) in thermal equilibrium

MAIN Phenomena:  
IONIZATION + RECOMBINATION  
EXCITATION (Dissociation)+ DE-EXCITATION (Light emission)





Simple picture:

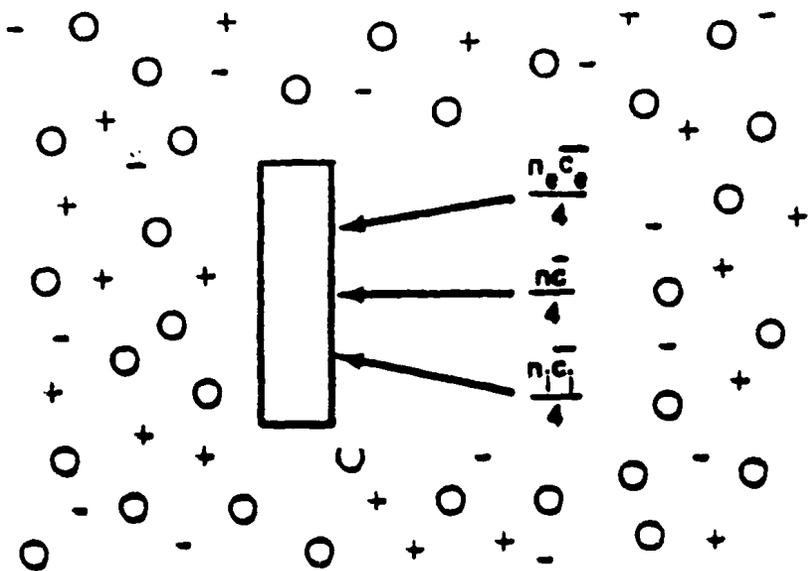
- Electron gas in thermal equilibrium
- Ion Gas in thermal equilibrium
- Neutral gas (obviously) in thermal equilibrium

For the three systems we define the energy distribution function.  
So we define an average energy (average temperature  $T$ ,  $T_i$ ,  $T_e$ )

For electron the average energy is 1 to 10 eV  
For gas and ions is of order of 0.1 eV.

A non perturbed plasma is defined by the condition  $N_i=N_e$

Typical values of  $N_i$  and  $N_e$  are in the range  $10^8$  to  $10^{12}$  ions(electrons)/cm<sup>3</sup>



Initial particle fluxes at the substrate

Neutrals

$$m = 6.6 \cdot 10^{-23} \text{g}$$

$$T = 20^\circ \text{C} = 293 \text{K} \equiv 1/40 \text{eV}$$

$$\bar{c} = 4.0 \cdot 10^4 \text{ cm/sec}$$

Ions

$$m_i = 6.6 \cdot 10^{-23} \text{g}$$

$$T_i = 500 \text{K} \equiv 0.04 \text{eV}$$

$$\bar{c}_i = 5.2 \cdot 10^4 \text{ cm/sec}$$

Electrons

$$m_e = 9.1 \cdot 10^{-28} \text{g}$$

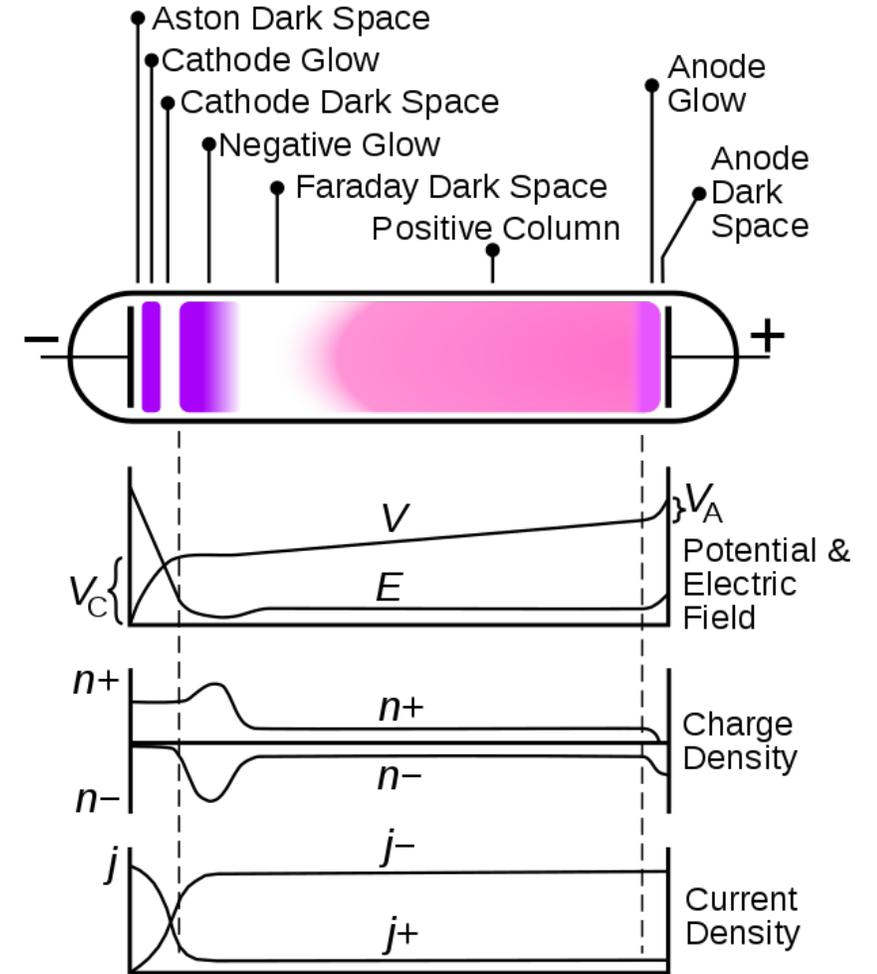
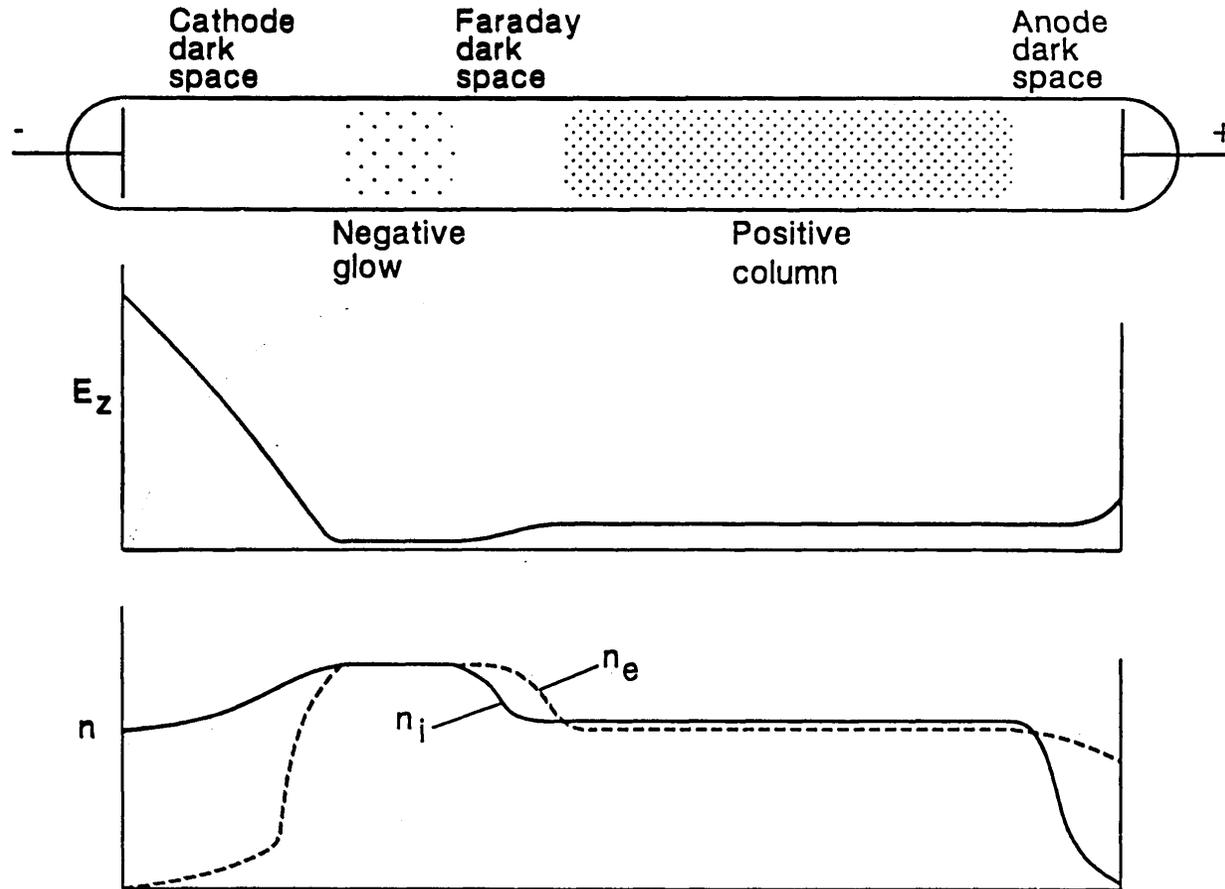
$$T_e = 23\,200 \text{K} \equiv 2 \text{eV}$$

$$\bar{c}_e = 9.5 \cdot 10^7 \text{ cm/sec}$$

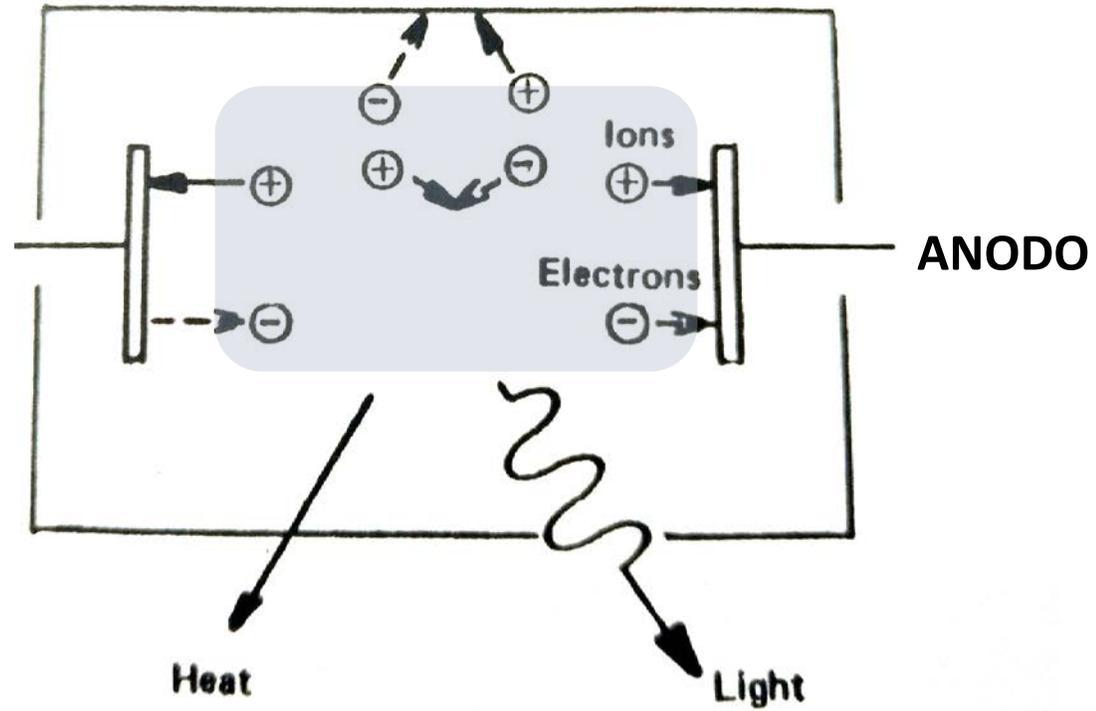
$$\bar{c} = \left( \frac{8kT}{\pi m} \right)^{1/2}$$



# Plasma Ignition between two electrodes in a rarefied gas

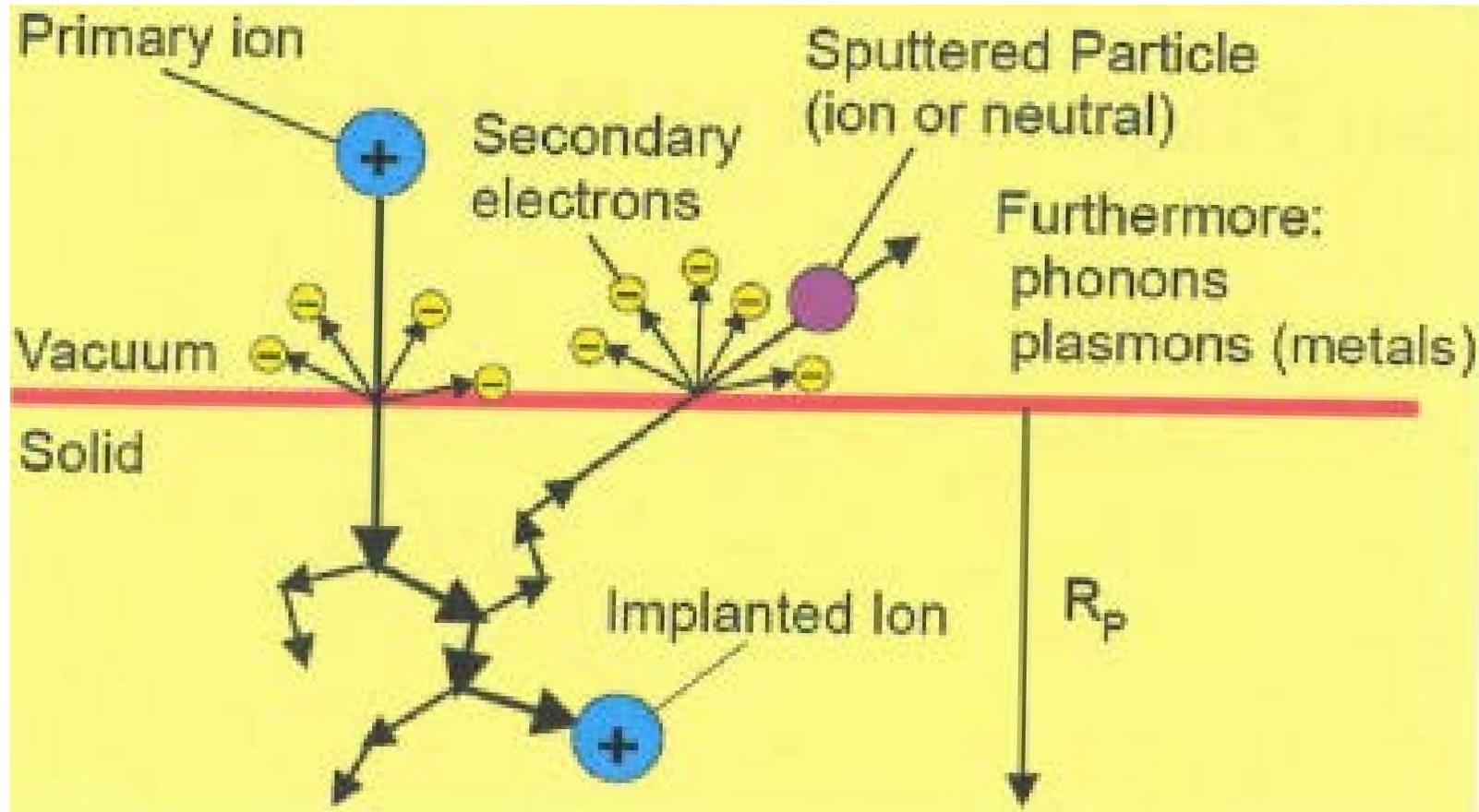


**CATODO**  
**Es: -500V**  
**Rispetto**  
**massa**



# COME USARE UN PLASMA PER DEPOSITARE MATERIALI INNOVATIVI ( ... E TRADIZIONALI)

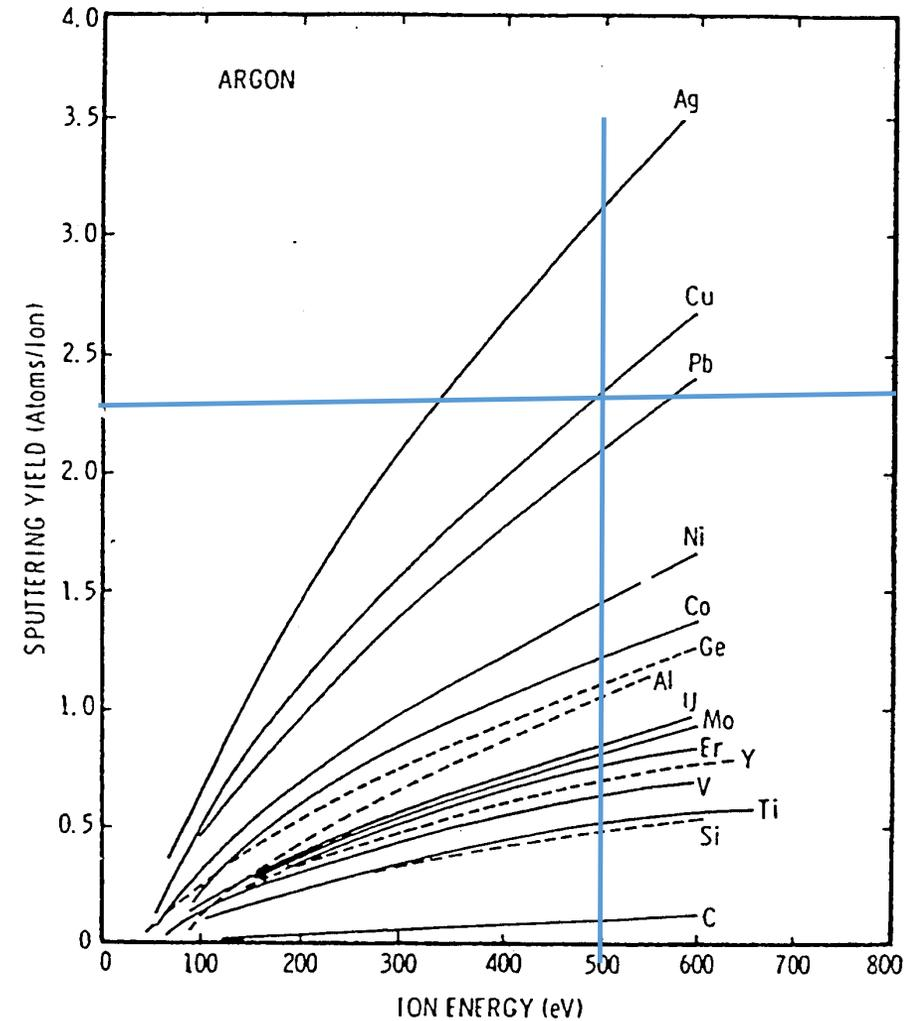
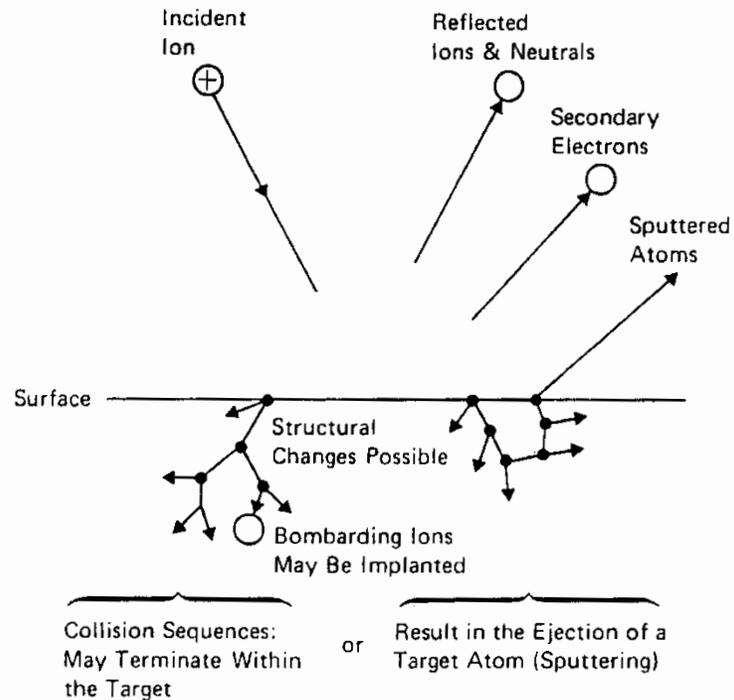
# IL FENOMENO FISICO DI SPUTTERING



# Sputtering: basic phenomena and experimental data

## What Is Sputtering?

Sputtering is a process operating on an atomic or molecular scale whereby an atom or molecule of a surface is ejected when the surface is struck by a fast incident particle (Figure 2). The process of sputtering is reasonably well understood. The momentum of the incident atom is transferred to the atoms in the target material and this momentum transfer can often lead to the ejection of a surface atom – the sputtering process. The process is often likened to a game of atomic snooker since the scattering process employs similar mechanics.



# MONTE CARLO TRIM CALCULATION

## INTERACTIONS OF IONS WITH MATTER

This website contains software on TWO Topics:

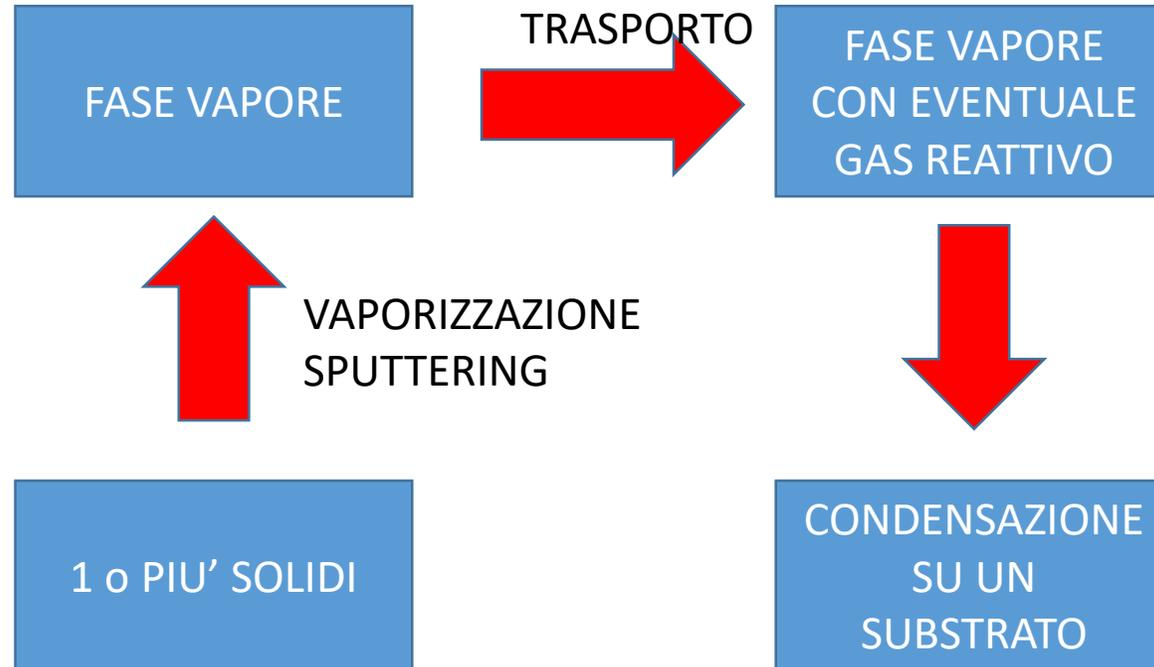
[SRIM - The Stopping and Range of Ions in Matter](#)

[SER - Soft Error Rates from Cosmic Rays](#) (see bottom of this page)

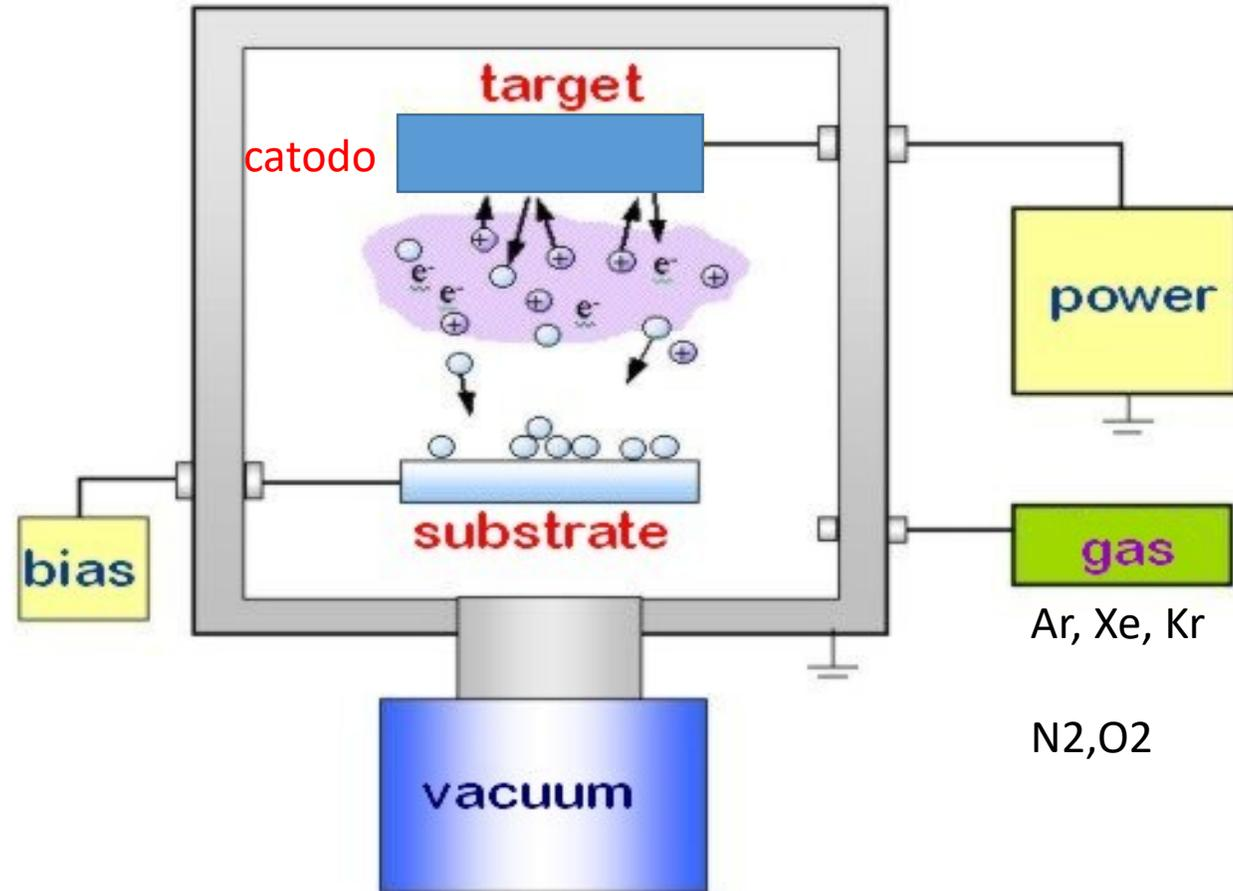
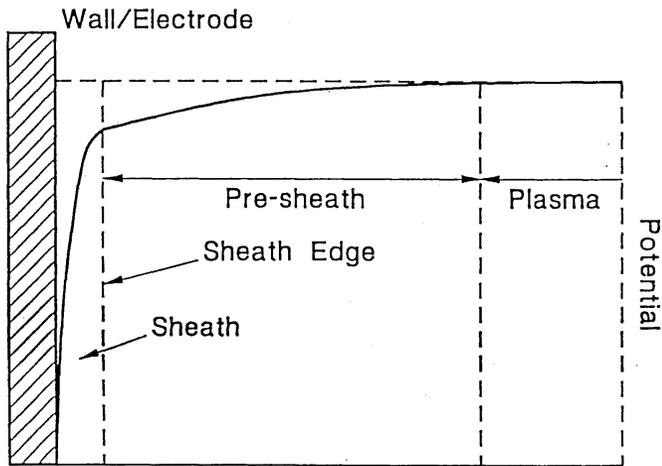
- <http://srim.org/>

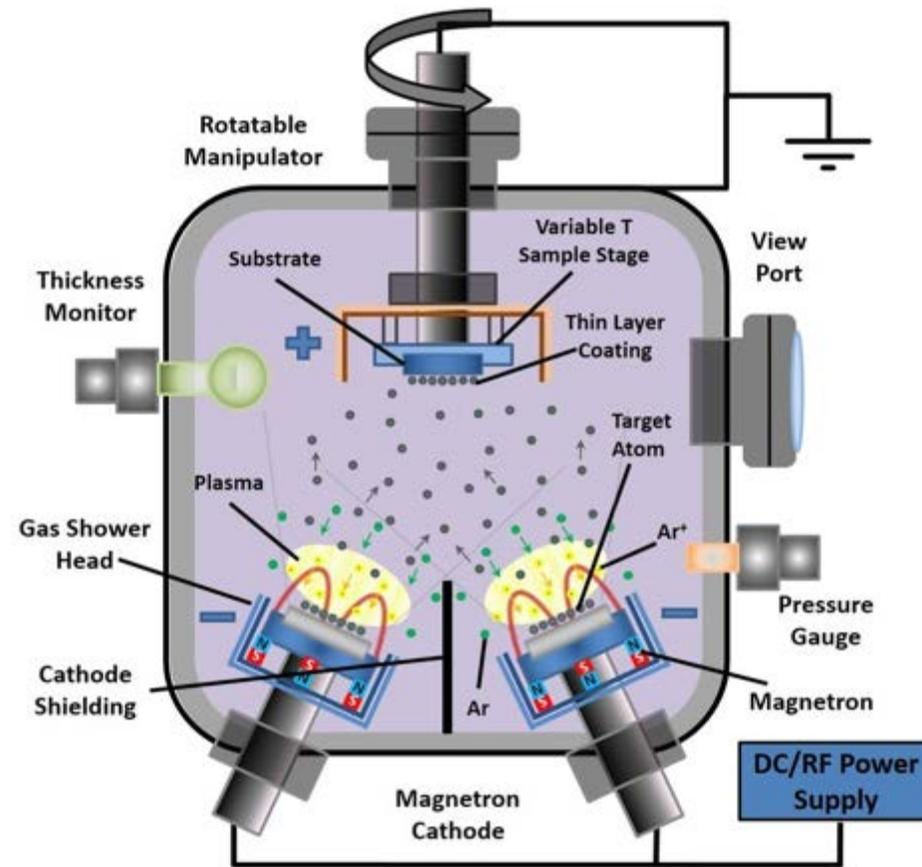
<b>NEW ! 100 Years of Ion Stopping</b> 2300+ Papers Listed and Results Plotted !!	
<b>SRIM Textbook</b>	
<b>ê Software ê</b>	<b>ê Science ê</b>
SRIM / TRIM Introduction	Historical Review
<b>Download SRIM-2013</b>	<b>Details of SRIM-2013</b>
SRIM Install Problems	Stopping in Compounds
SRIM Tutorials	High Energy Stopping Theory & Experiments
Download TRIM Manual Part-1, Part-2	Ranges of Ions
Stopping, Range and Damage by Neutrons	Including SRIM in Other Software Programs
<b>SRIM - Supporting Analytic Software</b>	<b>SREM - Stopping and Range of Electrons</b>

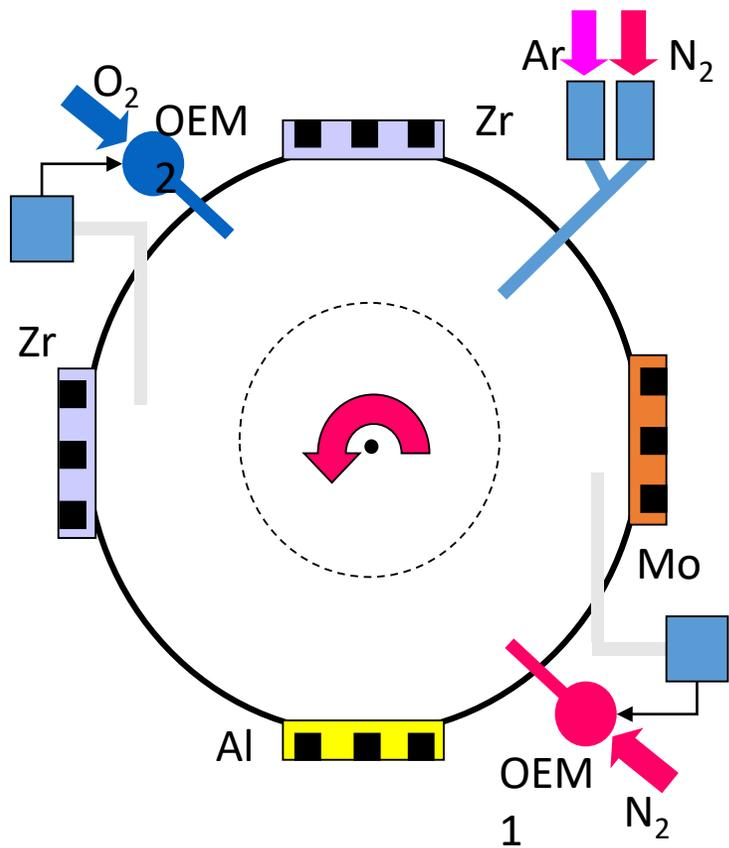
# From solid to vapor and back



# A simple sputtering system

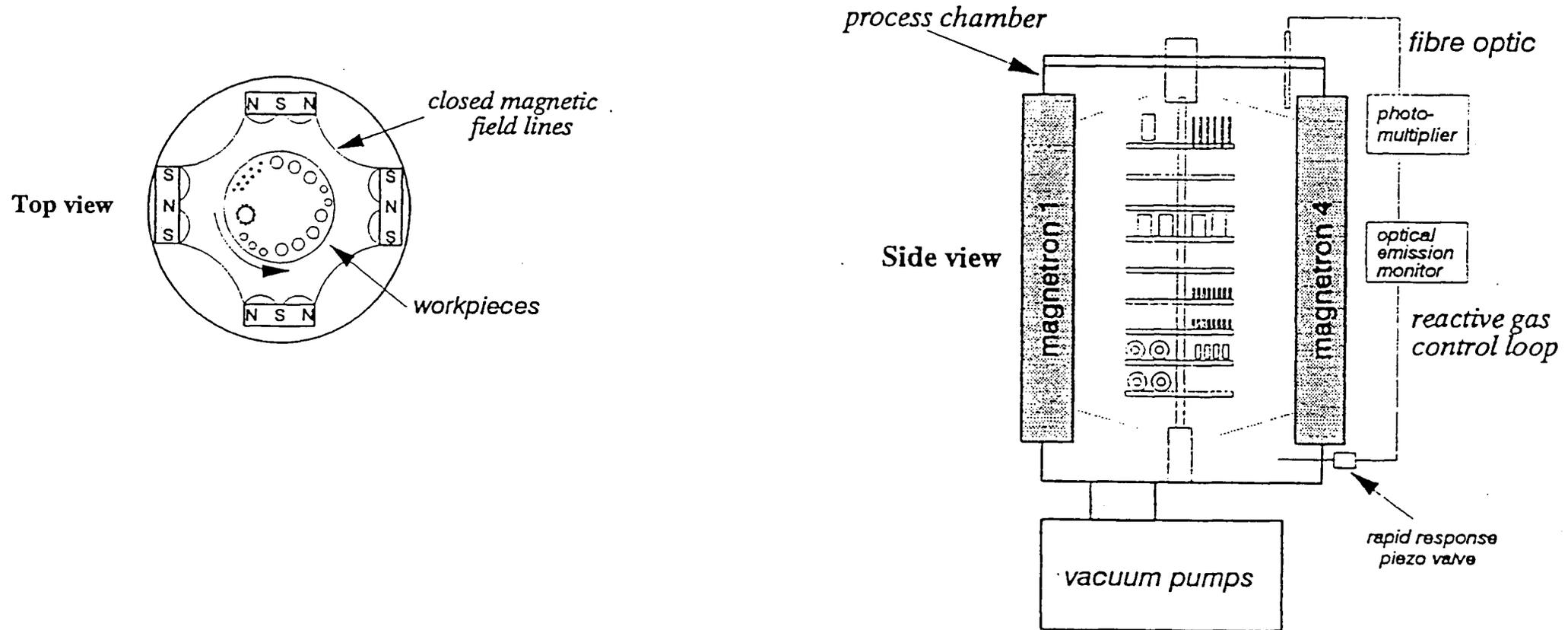






Teer Coatings (UK)

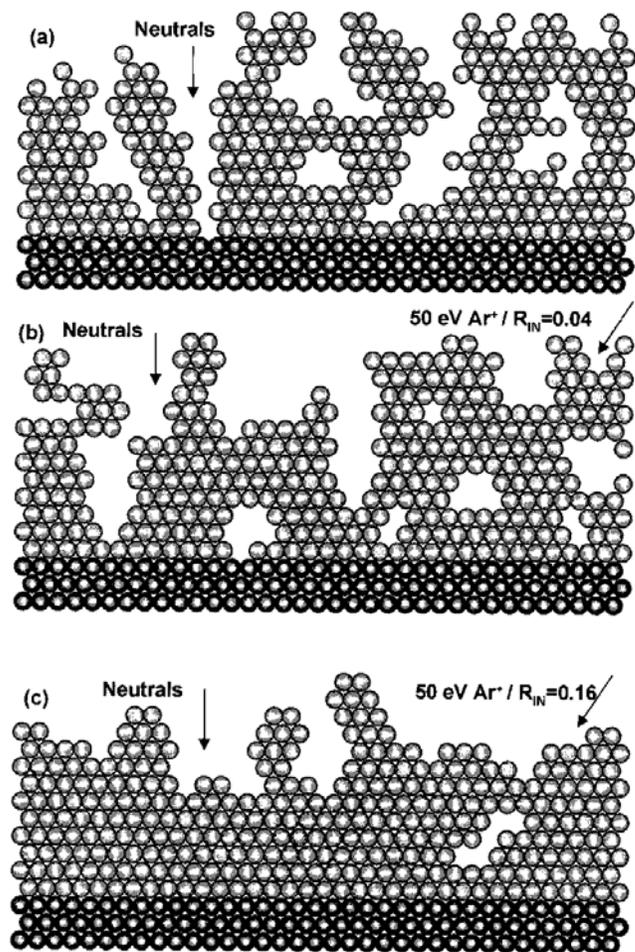
# 4 TARGETS CLOSED FIELD SYSTEM



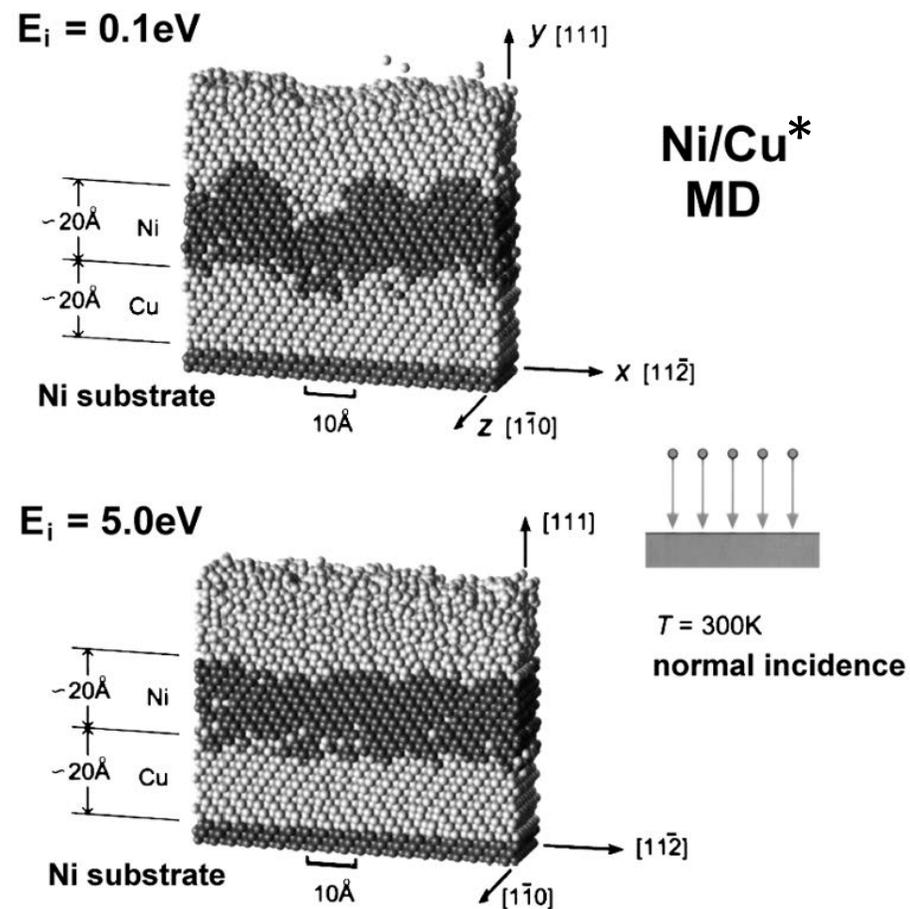
# Deposition of Thin Films by sputtering



# Deposition of Thin Films by sputtering: Ion Assisted growth

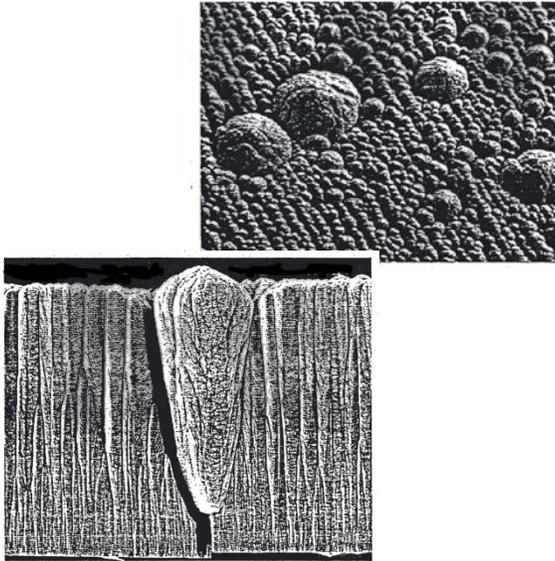


Morphology of a growing metal film as obtained from an early two-dimensional MD computer simulation using a Lennard-Jones interatomic potential, (a) without ion bombardment, (b) and (c) for IBAD using Ar<sup>+</sup> ions at  $E_i=50$  eV and  $R_{IN}=0.04$  and  $0.16$ , respectively. The directions of the incoming neutral and ion fluxes are indicated by arrows;



\* X. W. Zhou and H. N. G. Wadley, Journal of Applied Physics **87**, 2273 (2000).

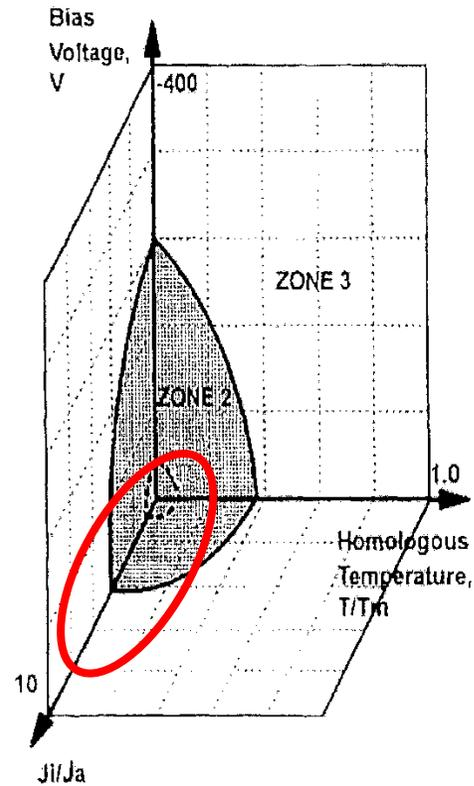
## Deposition of Thin Films by sputtering: Highlights on film growth



Effetto della temperatura

Effetto della pressione del gas

# Effetto del bombardamento ionico a bassa energia



Thornton

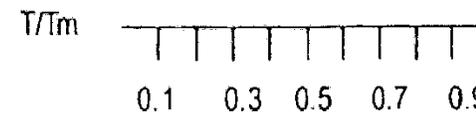
1	T	2	3
---	---	---	---

Messier

1	T	2	3
---	---	---	---

Kelly e Arnell

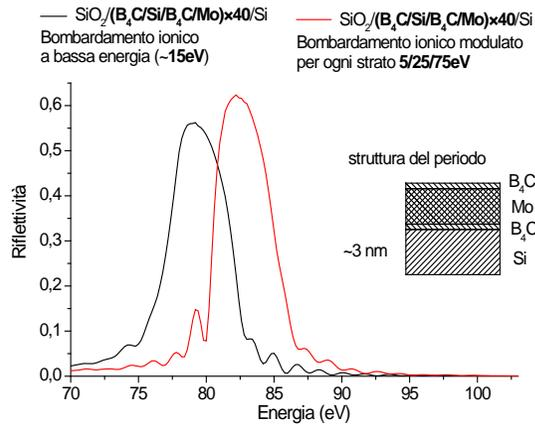
	2	3	
--	---	---	--



# Multilayer Mirrors

- Design and preparation of EUV and X-Ray High Reflectance Multilayer mirrors on flat and curved substrates for applications in astrophysics, lithography, “water-window” microscopy and Free Electron Laser Optics

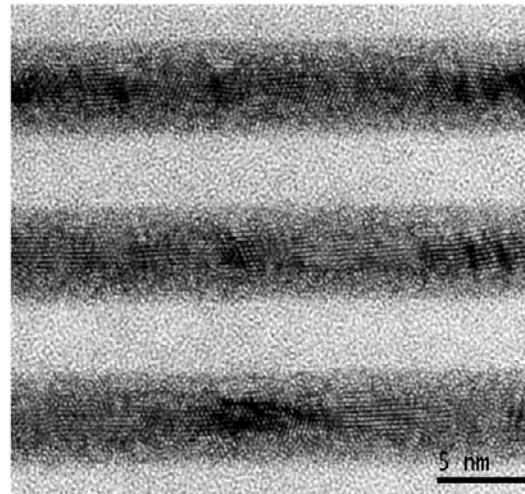
## EUV Bragg High Reflectivity



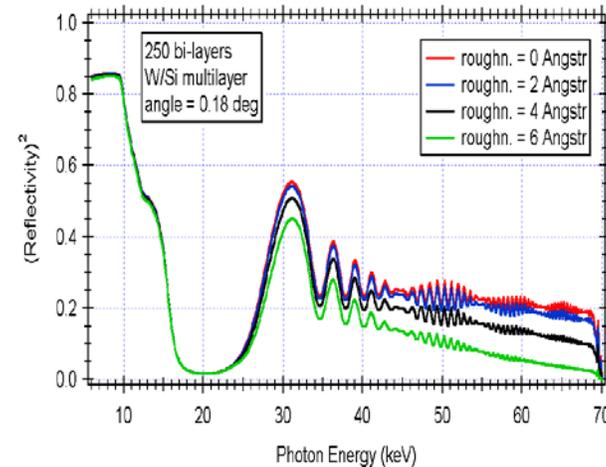
### EUV lithography mirrors

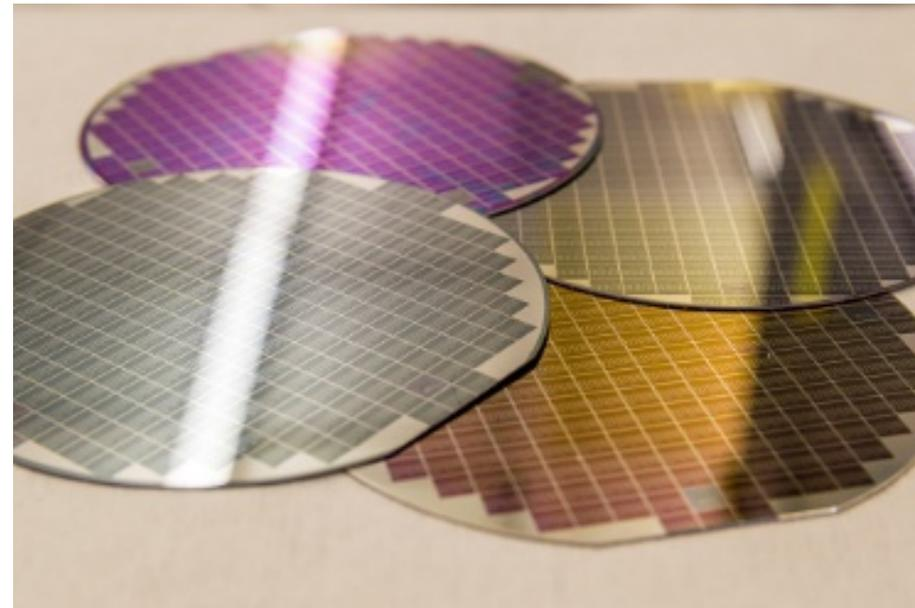
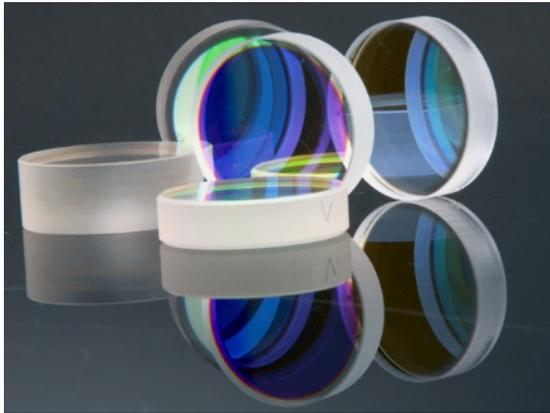
- “water-window” microscopy
- Free Electron Laser Optics
- EUV Polarimeters

## Multilayer Technology



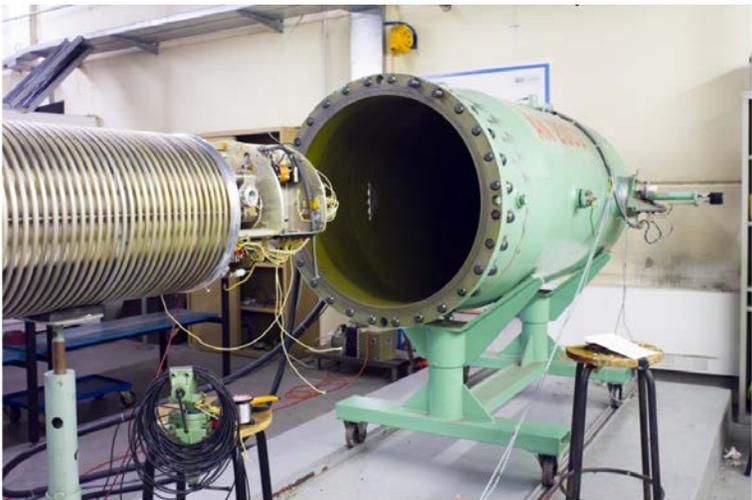
## Supermirror design for hard X-ray telescopes (Simbol-X)



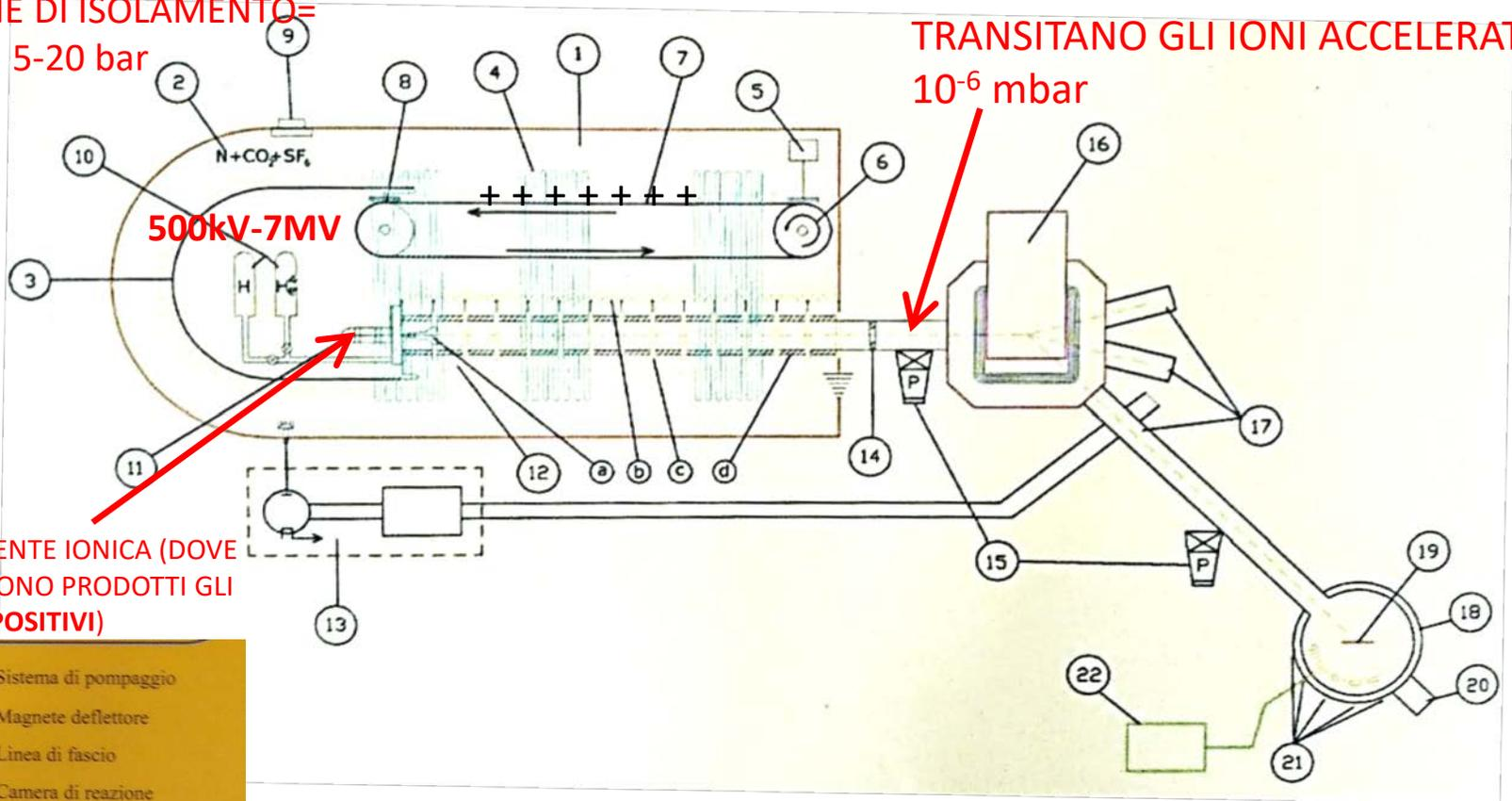




# ACCELERATORE VAN DE GRAAFF



PRESSIONE DI ISOLAMENTO=  
5-20 bar



PRESSIONE DEI TUBI ENTRO CUI  
TRANSITANO GLI IONI ACCELERATI:  
 $10^{-6}$  mbar

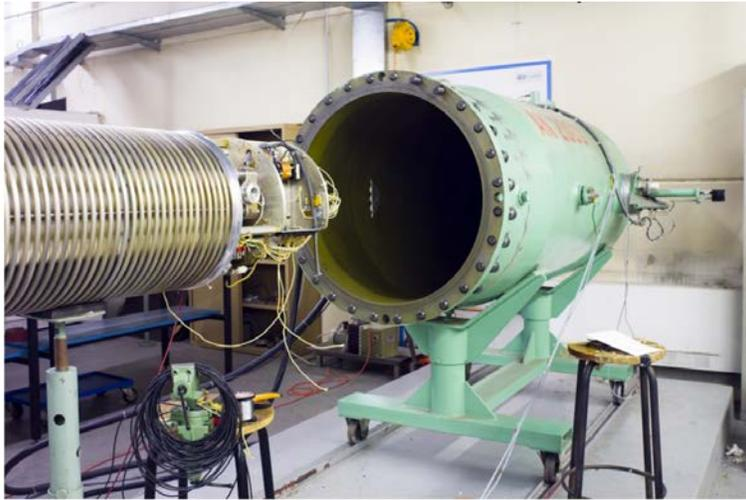
SORGENTE IONICA (DOVE  
VENGONO PRODOTTI GLI  
IONI POSITIVI)

- |                                  |                               |                         |
|----------------------------------|-------------------------------|-------------------------|
| 1 Tank                           | 10 Ampolle di gas             | 15 Sistema di pompaggio |
| 2 Gas di riempimento             | 11 Sorgenti di ioni           | 16 Magnete deflettore   |
| 3 Testa (term. H.V.)             | 12 Tubo acceleratore con:     | 17 Linea di fascio      |
| 4 Anelli di sostegno             | a Elettrodo di fuoco          | 18 Camera di reazione   |
| 5 Alimentatore di cariche        | b Partitore di tensione       | 19 Bersaglio            |
| 6 Motore                         | c Anelli focalizzanti         | 20 Pozzo di Faraday     |
| 7 Cinghia                        | d Elementi isolanti           | 21 Rivelatori           |
| 8 Pettine (Elettrodo di scarica) | 13 Sistema di stabilizzazione | 22 Acquisizione dati    |
| 9 Voltmetro                      | 14 Anello di Fuoco            |                         |

**MICROANALISI  
IMPIANTAZIONE IONICA  
LITOGRAFIA IONICA  
IRRAGGIAMENTI**

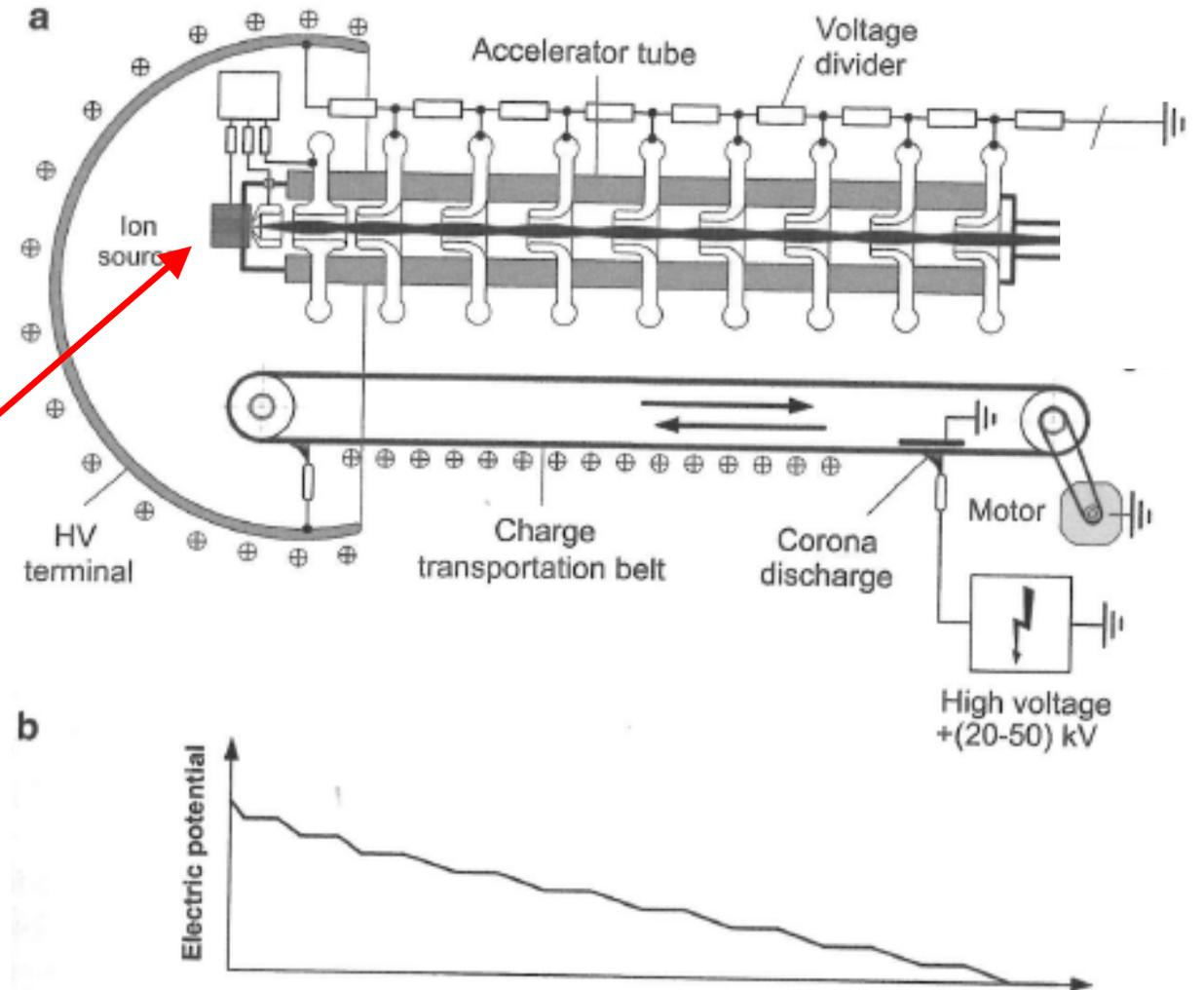
# ACCELERATORE VAN DE GRAAFF

PRESSIONE DI ISOLAMENTO= 5-20 bar

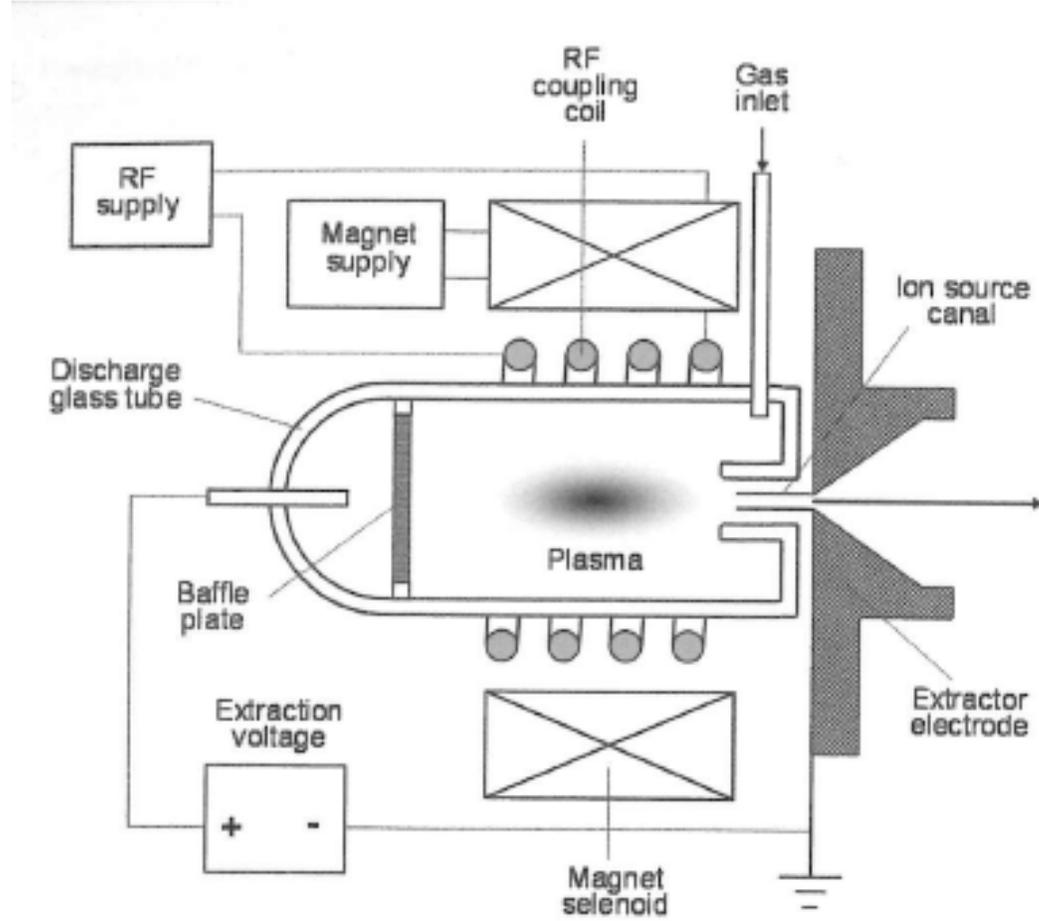


500kV-7MV

SORGENTE IONICA (DOVE VENGONO PRODOTTI GLI IONI POSITIVI)



Scheme of the Van de Graaff generator (a) and (b) the accelerating potential

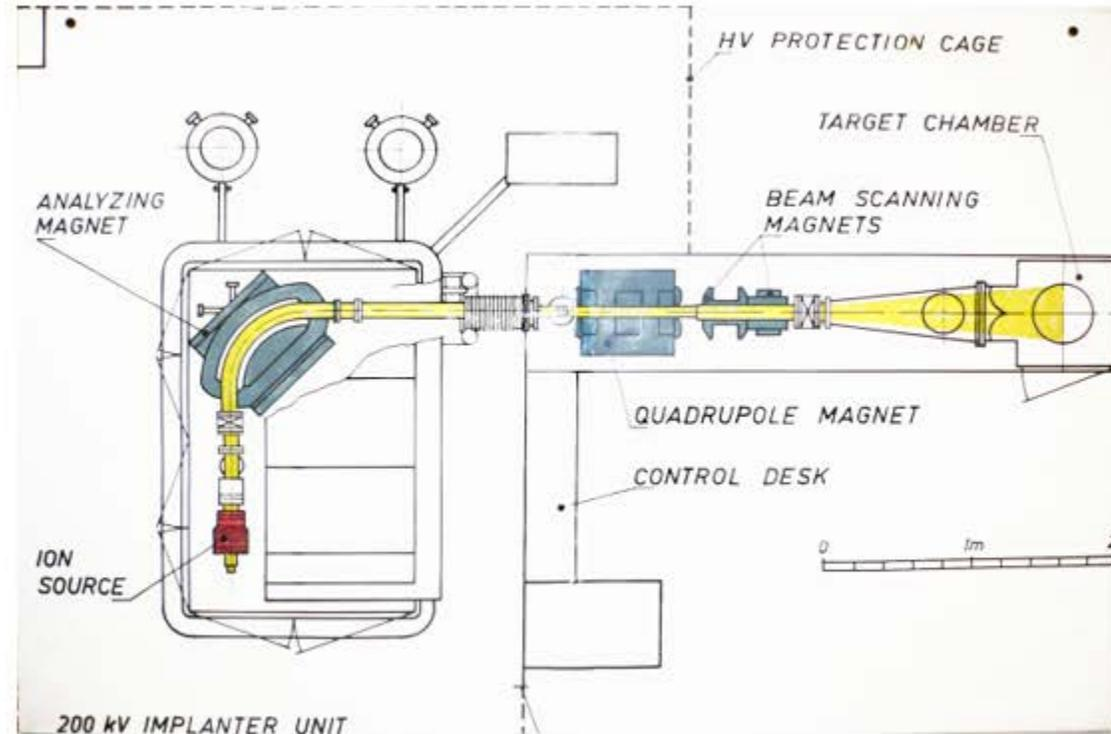


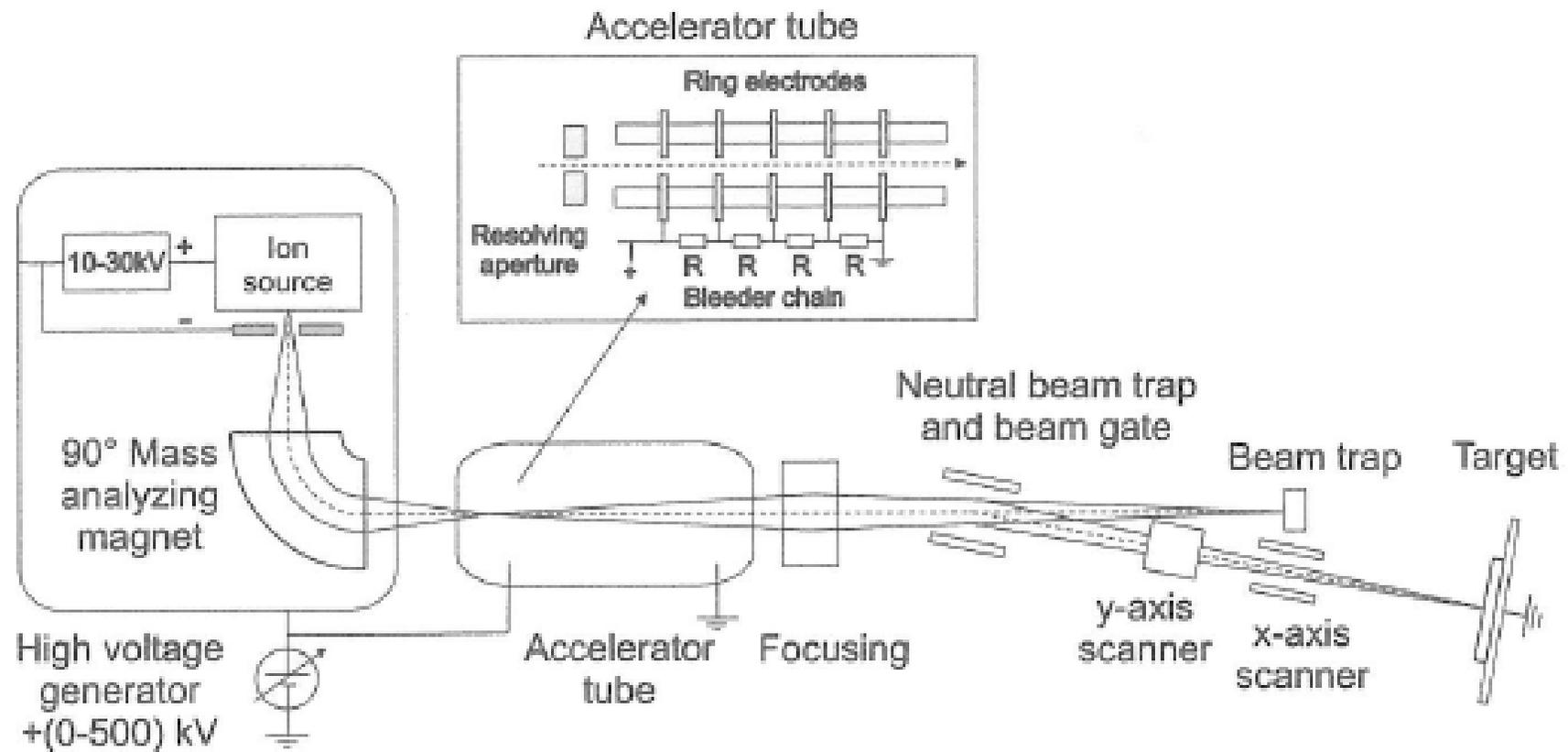
Principal buildup of a radio-frequency ion source

# IMPIANTATORE IONICO

## Ion Implantation ( $V < 200\text{KV}$ )

- ❑ Surface modification (H, Ar, Xe...)
- ❑ Doping of semiconductor
- ❑ Metal ions implantation (Au, Ag, Cu, Ga, Ni, Co, Fe, N, As ..)
  - optical properties
  - nano-clusters
  - alloys formation
- ❑ ion mixing





Principal technical buildup of low energy ion accelerators (ion implanter)

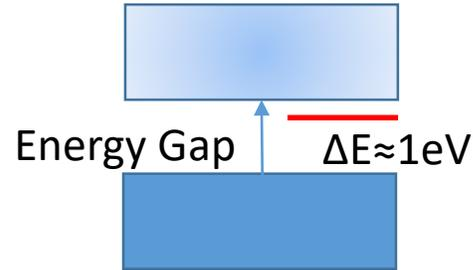
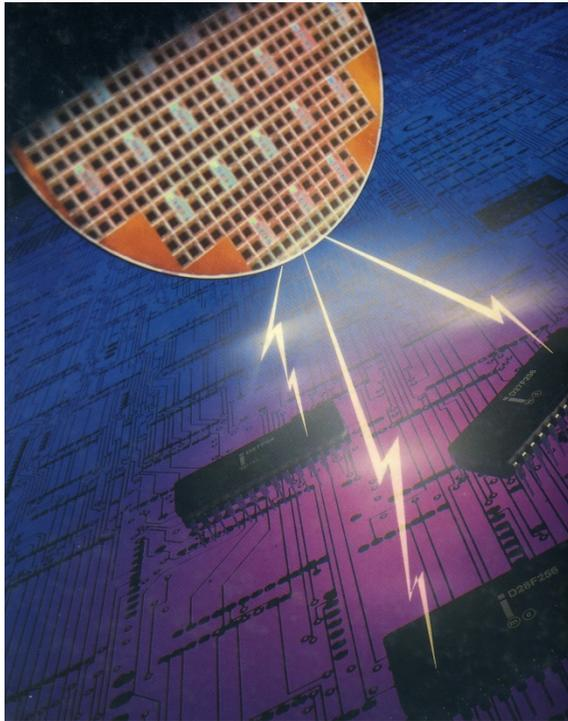
# SEMICONDUTTORI (CENNI)

## SOLIDI CRISTALLINI



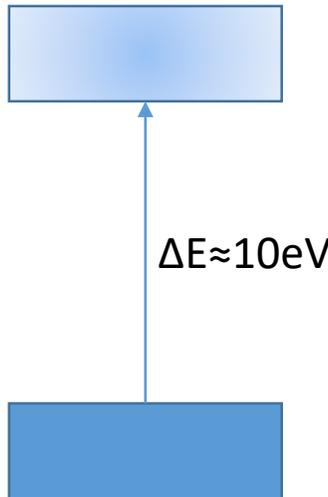
## CONDUTTORI

Appartengono a questa categoria tutti i metalli, come, ad esempio, rame (Cu), argento (Ag), Alluminio (Al). Sono ottimi conduttori sia di corrente che di calore e possiedono una struttura cristallina. La conducibilità elettrica diminuisce con la temperatura in un ampio range di temperature.



## SEMICONDUTTORI

Le loro proprietà sono intermedie tra quelle dei conduttori e degli isolanti. Sono sostanze solide cristalline (come il Silicio, Germanio e Diamante) che offrono conducibilità crescente all'aumentare della temperatura. A temperatura ambiente manifestano proprietà di conduzione elettrica dovute ad impurezze perché elettroni possono passare alla banda di conduzione (per eccitazione termica  $3/2kT$  o per fotoeccitazione= esposizione alla luce visibile). La conducibilità elettrica aumenta con la temperatura. L'aggiunta di opportune impurità può esaltare la conduzione elettrica (drogaggio dei semiconduttori)

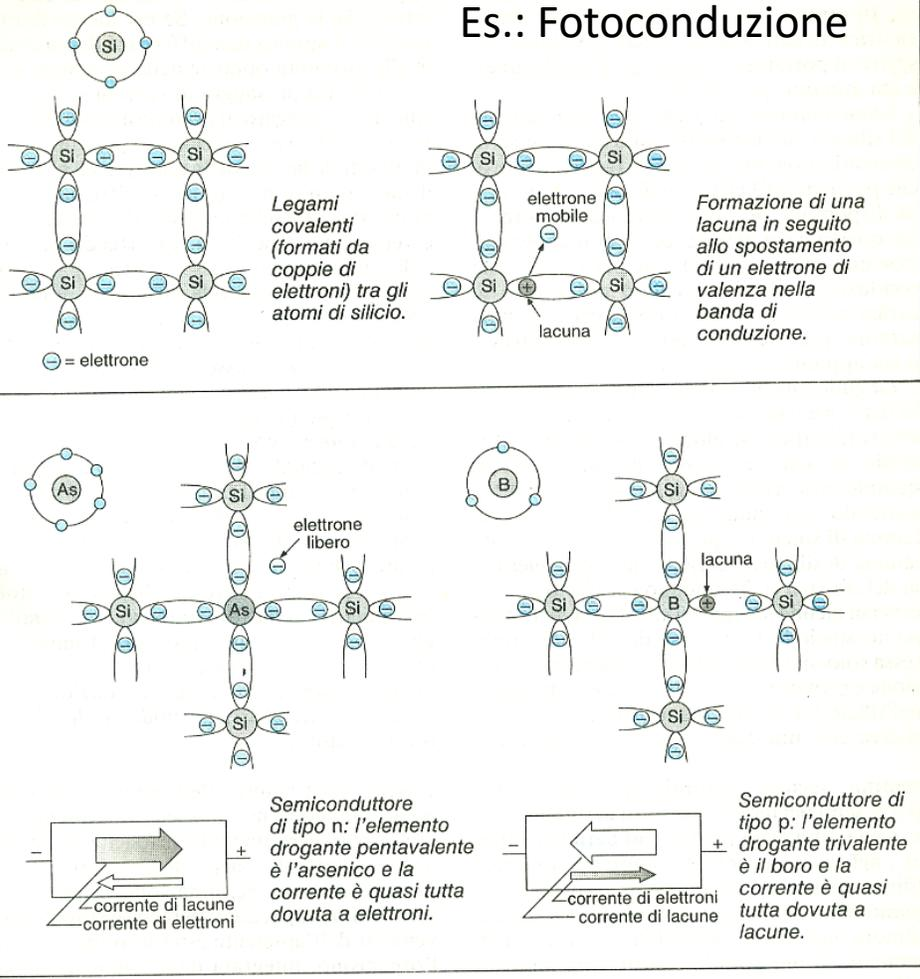


## ISOLANTI

Lo sono principalmente solidi ionici e covalenti. In un isolante non esistono elettroni di valenza liberi di muoversi e tali da evidenziare un flusso di cariche ordinate, sotto l'azione di un campo elettrico. Queste sostanze sono definite isolanti perché offrono una resistenza assai grande al passaggio di cariche elettriche.

Resistività ( $\Omega\text{cm}$ )	Materiale
$\rho < 10^{-3}$	Metalli
$10^{-3} < \rho < 10^5$	Semiconduttori
$\rho > 10^5$	Isolanti

## Es.: Fotoconduzione



La caratteristica principale delle tecnologia dei circuiti integrati è il controllo della conducibilità elettrica del Silicio, ottenuta mediante la introduzione controllata di elementi elettricamente attivi nel reticolo cristallino.

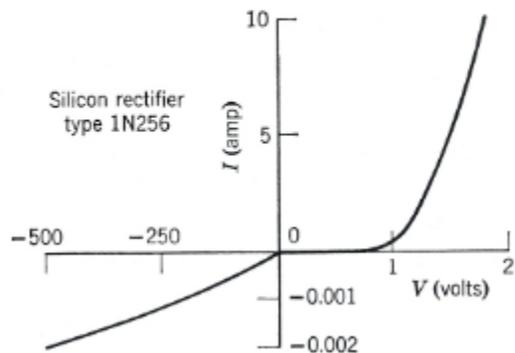
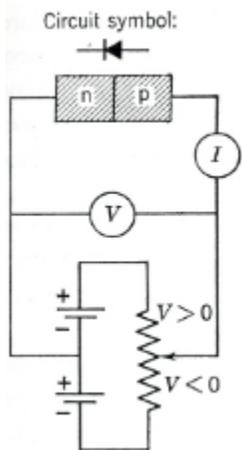
Elementi della colonna III (come il Boro (B) o della colonna V (come il fosforo (P) e Arsenico (As) possono essere introdotti nel semiconduttore (colonna IV) nei siti reticolari. L'introduzione di detti atomi pentavaletti o trivalenti al posto di atomi (ad esempio) di silicio è conosciuta con il nome di DROGAGGIO:

Impurezze che comportano una deficienza di elettroni rendono il semiconduttore di tipo P (positivo)

III	IV	V
5 B Boron	6 C Carbon	7 N Nitrogen
13 Al Aluminum	14 Si Silicon	15 P Phosphorus
31 Ga Gallium	32 Ge Germanium	33 As Arsenic

Impurezze che «donano» elettroni rendono il semiconduttore di tipo N (negativo)

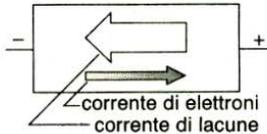
# DIODI E TRANSISTOR



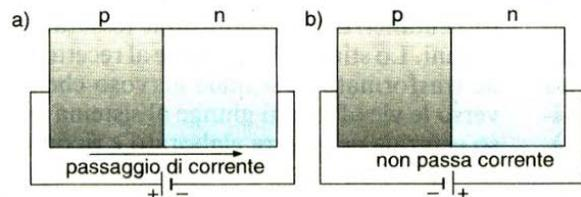
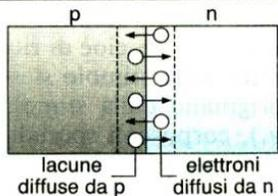
Semiconduttore di tipo n: l'elemento drogante pentavalente è l'arsenico e la corrente è quasi tutta dovuta a elettroni.



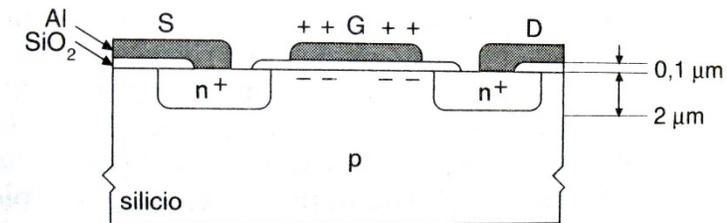
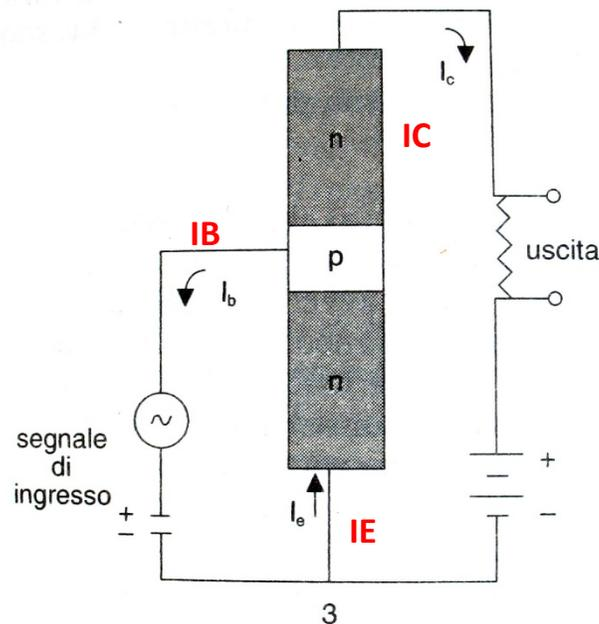
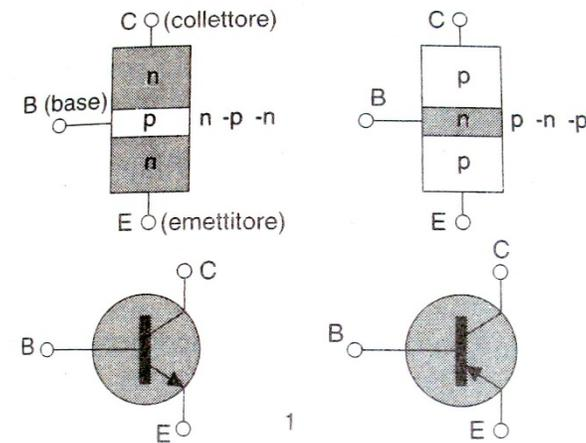
Semiconduttore di tipo p: l'elemento drogante trivalente è il boro e la corrente è quasi tutta dovuta a lacune.

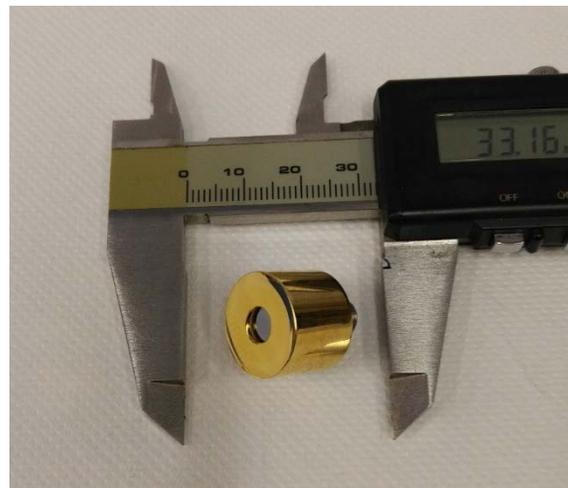
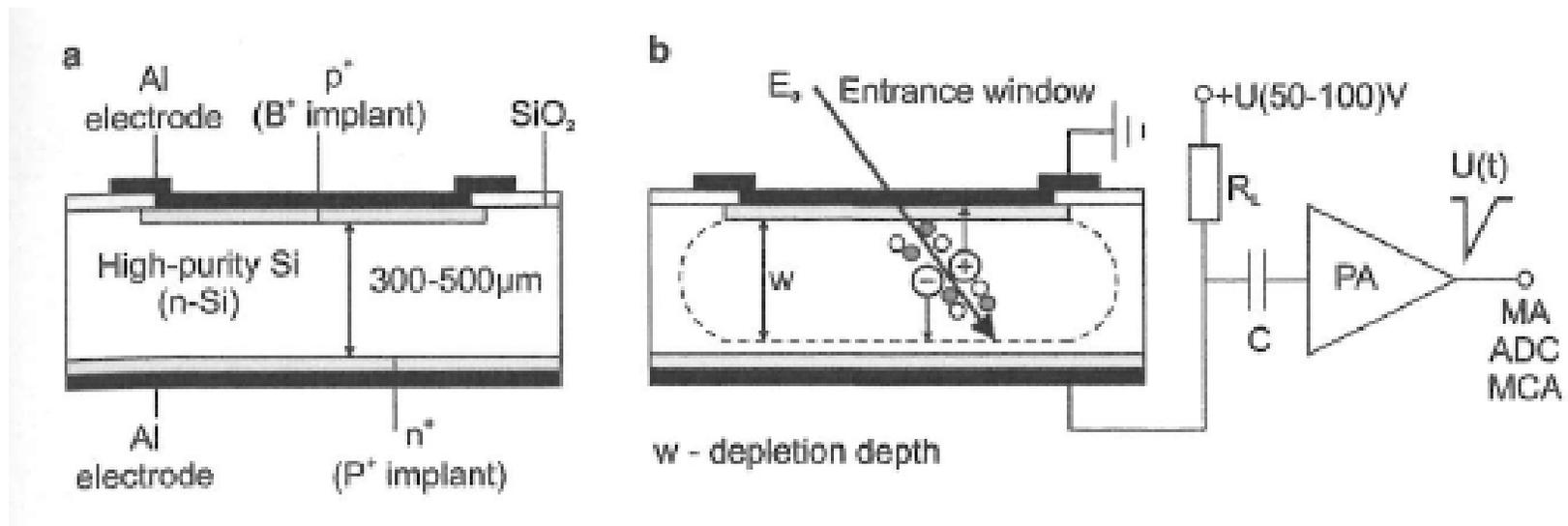


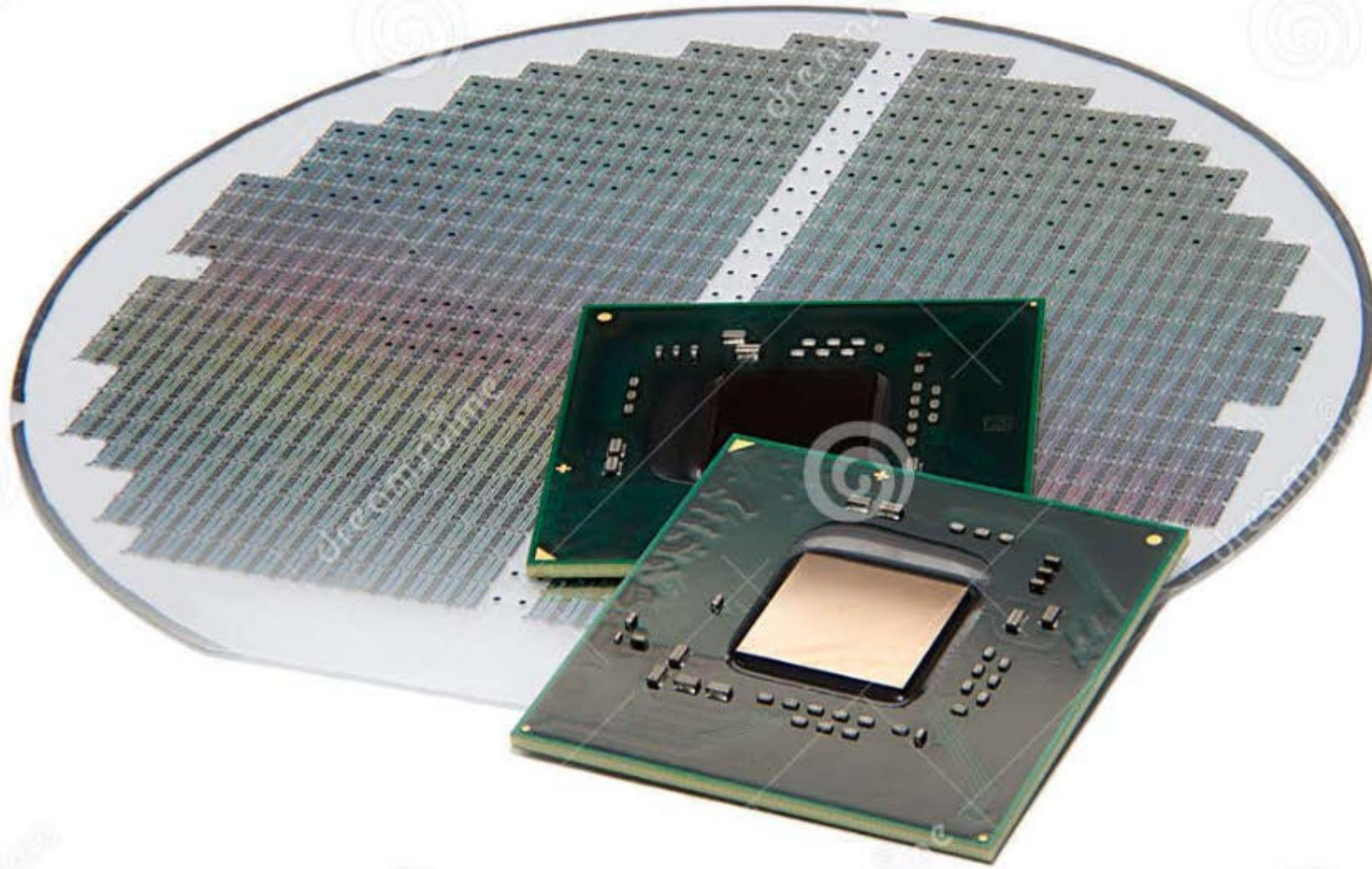
Nella giunzione p-n la diffusione di elettroni va da n a p, mentre le lacune diffondono nel verso opposto: la diffusione è circoscritta alla zona di giunzione e termina quando la differenza di potenziale creata si oppone a ogni ulteriore diffusione di cariche.



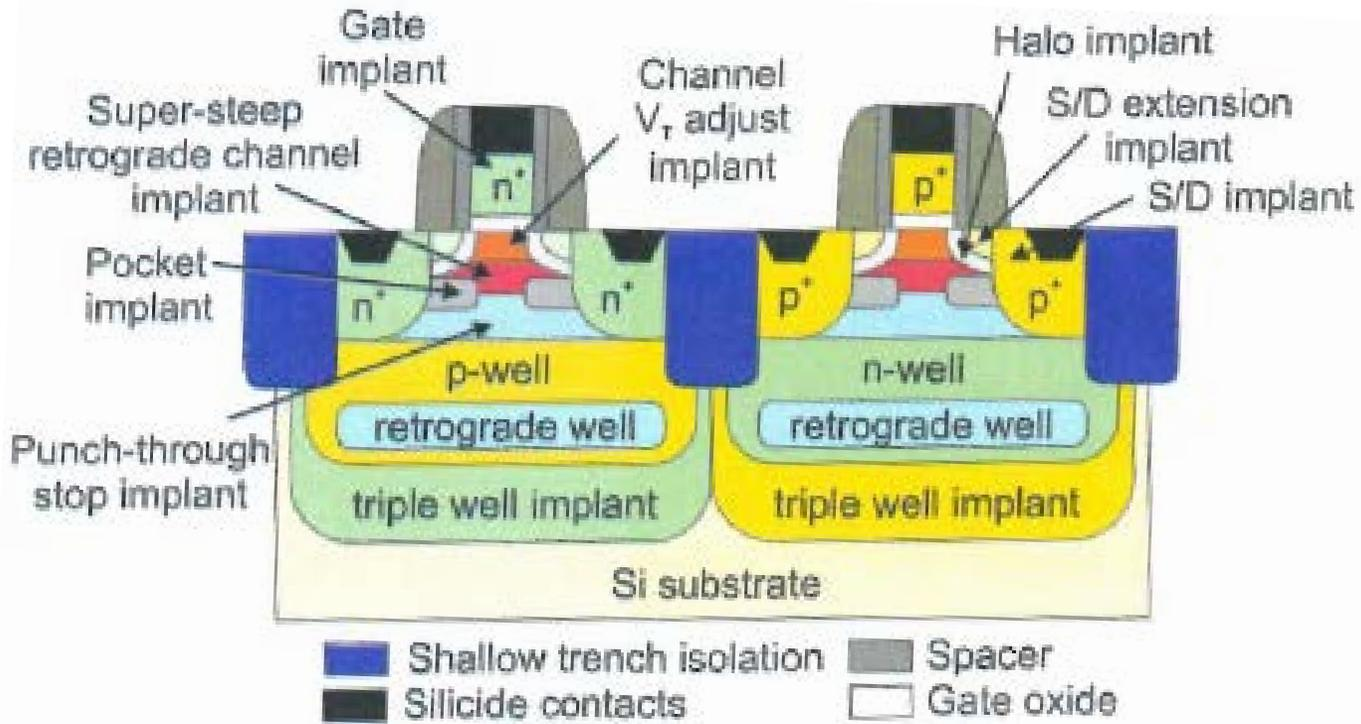
Un diodo a giunzione: il passaggio di corrente si ha solo se il semiconduttore p è collegato al polo positivo della pila (a); viceversa, invertendo i collegamenti, non passa corrente (b).











B Ion-implanted regions in a common CMOS transistor

Ion Fluence – energy of different ion implantation for silicon MOS devices and process technology

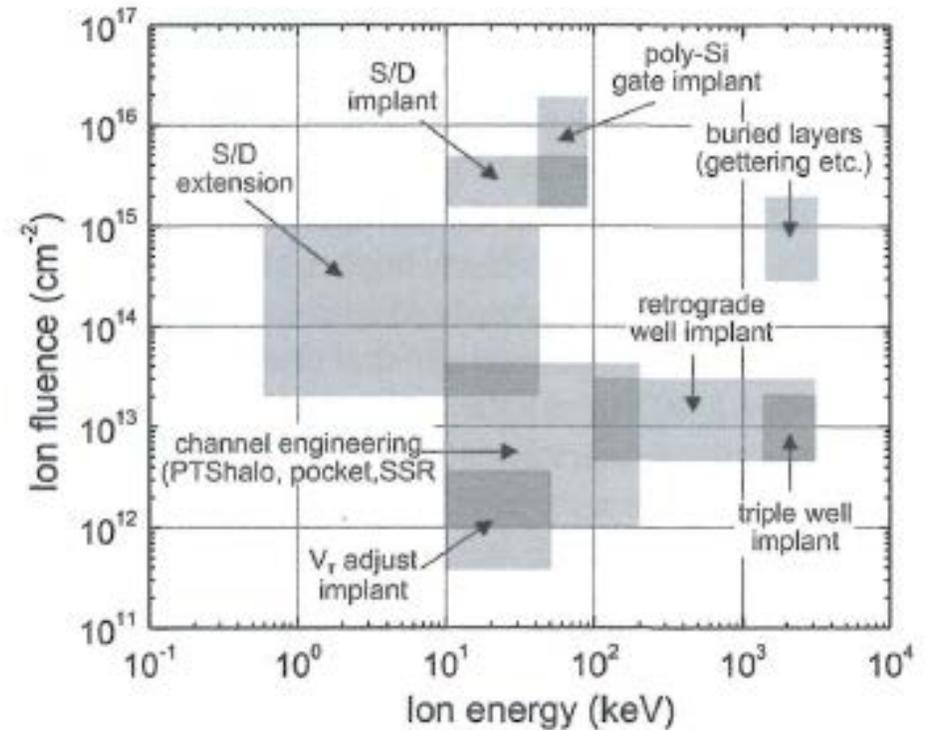


**Table 4.2** Implantation processes and parameters for advanced CMOS transistor technology

Transistor region	Ions	Energy (keV)	Fluence (cm <sup>-2</sup> )	Remarks
Channel formation	P, B	10–80	$1 \times 10^{12}$ – $5 \times 10^{13}$	Halo, PTS, LATIPS, Pocket, SSR
	As, In, Sb	80–200		High tilt angles and wafer re-depositioning
Transistor threshold voltage adjust	B, BF <sub>2</sub> , As	10–50	$4 \times 10^{11}$ – $4 \times 10^{12}$ ( $\rightarrow 1 \times 10^{11}$ )	Transistor threshold voltage
Source/drain deep contacts	As, BF <sub>2</sub> , B	10–80 ( $\rightarrow 1$ –30)	$2 \times 10^{15}$ – $8 \times 10^{15}$ ( $\rightarrow 1 \times 10^{15}$ – $4 \times 10^{15}$ )	Conducting source/drain areas
Source/drain extension	As, BF <sub>2</sub> , B	0.5–30	$3 \times 10^{13}$ – $1 \times 10^{15}$	Electric field reduction near S/D
poly-Si gate doping	B, BF <sub>2</sub> , P	30–80 ( $\rightarrow 2$ –30)	$3 \times 10^{15}$ – $2 \times 10^{16}$ ( $\rightarrow 1 \times 10^{15}$ – $8 \times 10^{15}$ )	Conducting gate material
Preamorphization	Ge, Si	5–50	$5 \times 10^{13}$ – $2 \times 10^{15}$	Channeling suppression
Retrograde wells	B, P	1,500–3,000	$5 \times 10^{12}$ – $3 \times 10^{13}$	Off-state leakage current reduction
Triple wells	P, B	1,200–3,000 ( $\rightarrow 5,000$ )	$5 \times 10^{12}$ – $3 \times 10^{13}$	p- and n-well separation
Buried layers	B, P	1,500–3,000	$2 \times 10^{13}$ – $5 \times 10^{13}$ , $3 \times 10^{14}$ – $2 \times 10^{15}$	Subcollector in bipolar transistors
Proximity gettering	C, N, O, F, Si	1,500–3,000	$5 \times 10^{14}$ – $5 \times 10^{15}$	Carrier lifetime improvement
SOI wafer fabrication	O	30–100	$3 \times 10^{16}$ – $1 \times 10^{17}$	SIMOX
	H, He			Smart-Cut

Isbn 978-3-211-99356-9

# ESEMPI CON SIMULAZIONI TRIM

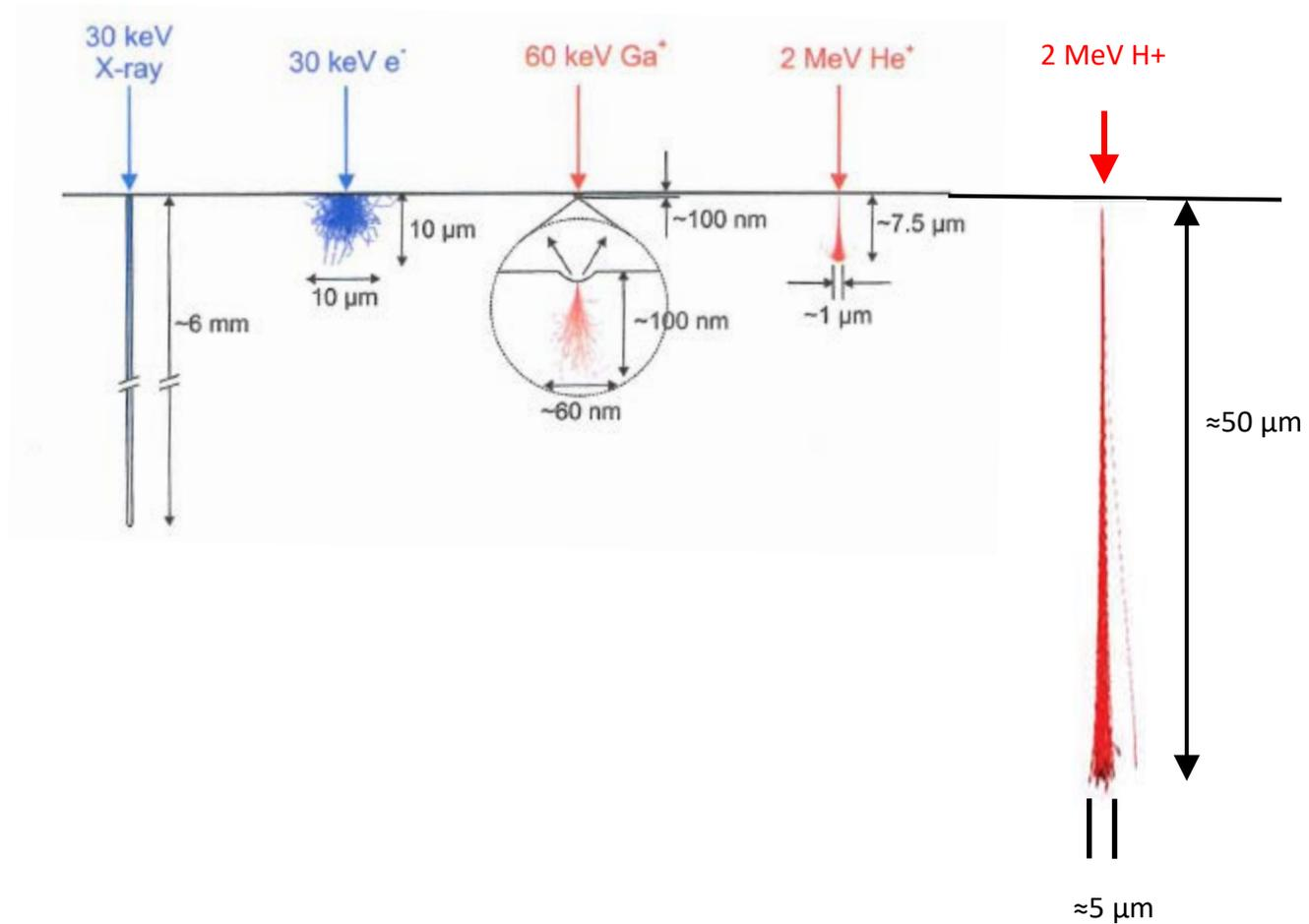
- Si può ottenere un drogaggio selettivo di un semiconduttore con controllo sulla profondità sulla scala di 10-100nm mediante acceleratori di ioni con energie da 10keV a 500keV
- Il controllo sulla posizione è demandato alle maschere ottenute con tecniche di foto-litografia e deposizione di film sottili.
  
- Si può modificare il materiale in profondità dell'ordine delle decine di micrometri con ioni leggeri dell'energia di qualche MeV

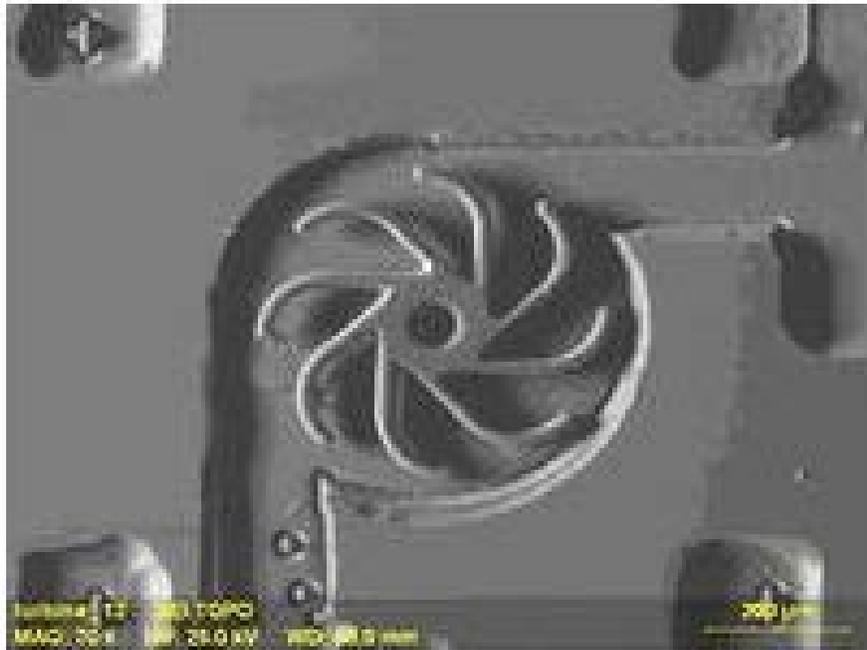


# Proton beam writing

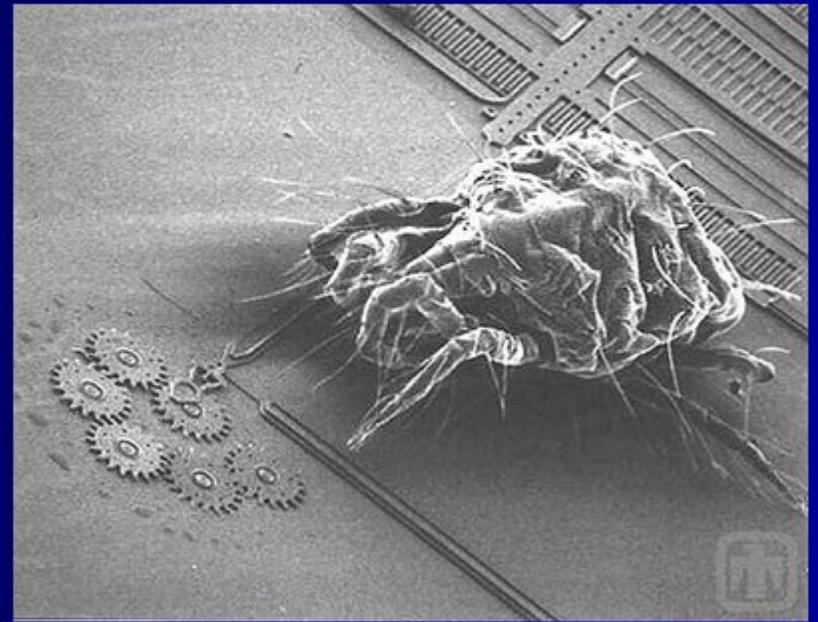
Proton beam (p-beam) writing is a new direct-writing process that uses a focused beam of MeV protons to pattern resist material at nanodimensions. The process, although similar in many ways to direct writing using electrons, nevertheless offers some interesting and unique advantages. Protons, being more massive, have deeper penetration in materials while maintaining a straight path, enabling p-beam writing to fabricate three-dimensional, high aspect ratio structures with vertical, smooth sidewalls and low line-edge roughness. Calculations have also indicated that p-beam writing exhibits minimal proximity effects, since the secondary electrons induced in proton/electron collisions have low energy. A further advantage stems from the ability of protons to displace atoms while traversing material, thereby increasing localized damage especially at the end of range. P-beam writing produces resistive patterns at depth in Si, allowing patterning of selective regions with different optical properties as well as the removal of undamaged regions via electrochemical etching.

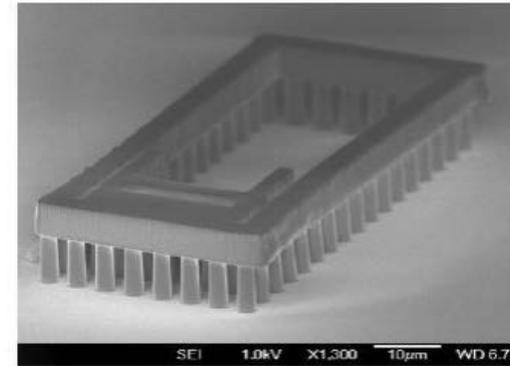
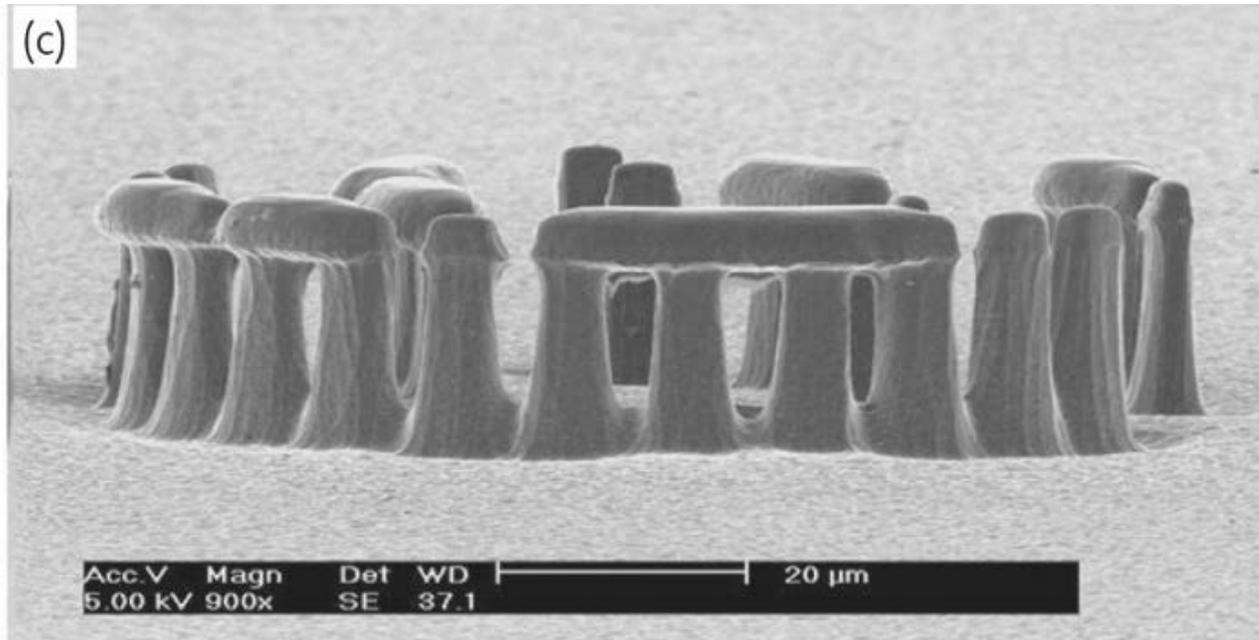
Frank Watt\*, Mark B. H. Breese, Andrew A. Bettioli, and Jeroen A. van Kan  
 Centre for Ion Beam Applications (CIBA), Physics Department, National University of Singapore, Singapore 117542  
 \*E-mail: [phywatt@nus.edu.sg](mailto:phywatt@nus.edu.sg)





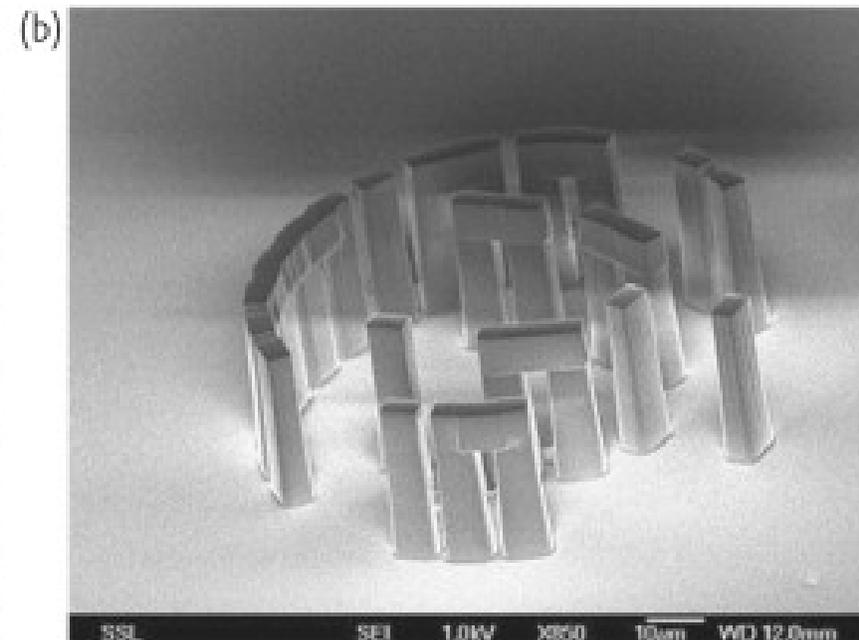
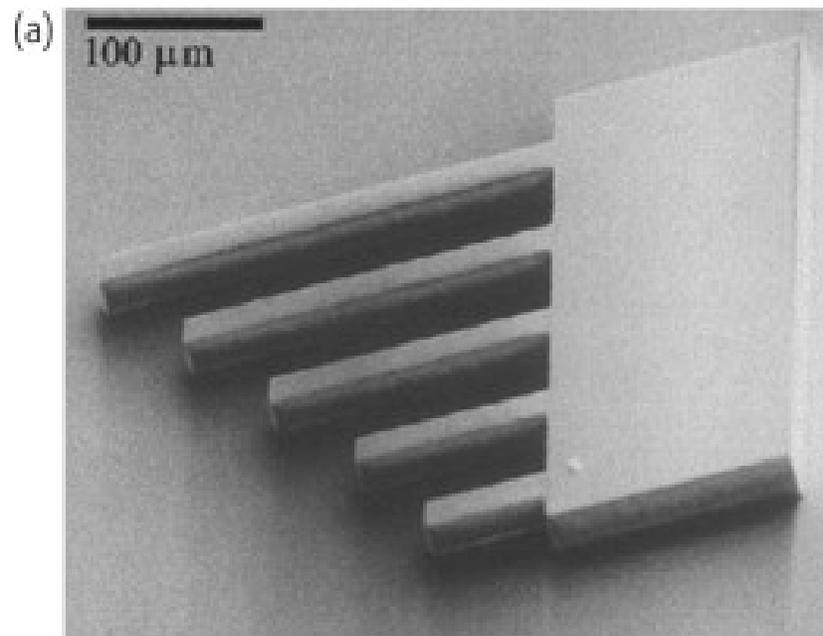
## Micromacchine: *componenti*

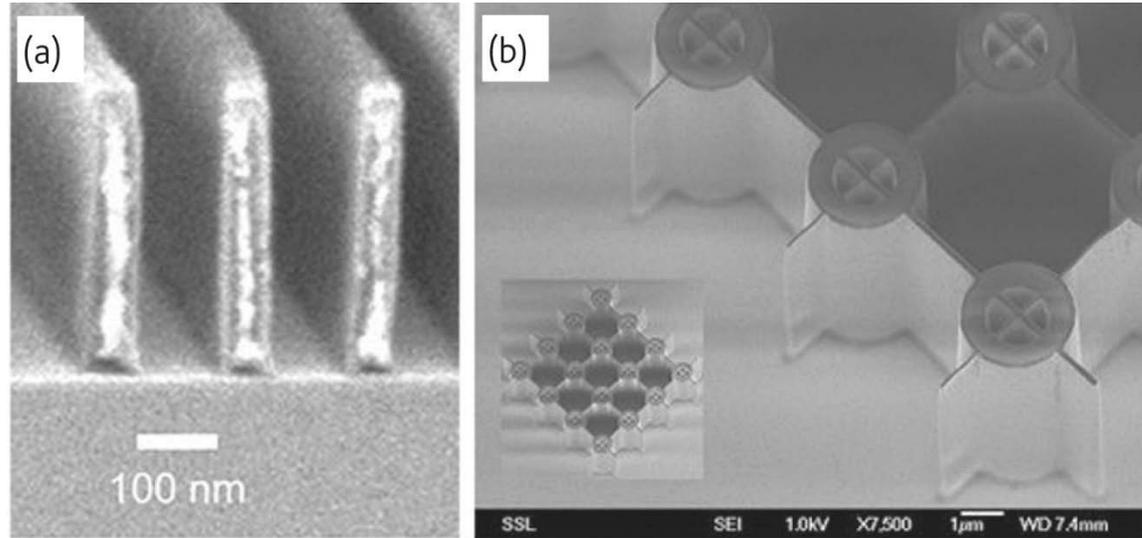




J. A. van Kan, P. G. Shao,  
K. Ansari, A. A. Bettiol,  
T. Osipowicz, F. Watt,  
Microsyst Technol 13 431(2007)

Parthenon's copy with a  
reduction of 1 million times

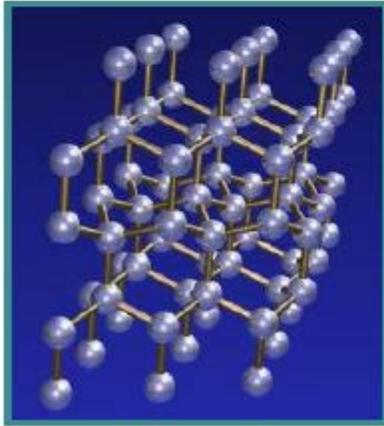




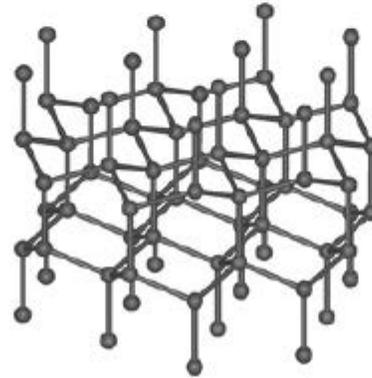
<https://www.sciencedirect.com/science/article/pii/S1369702107701293#fig1>

# Diamond

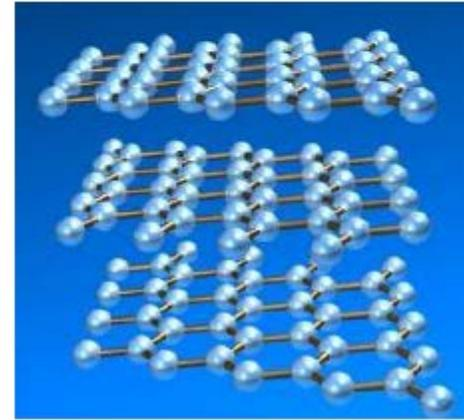
αδάμας (*indestructible*)



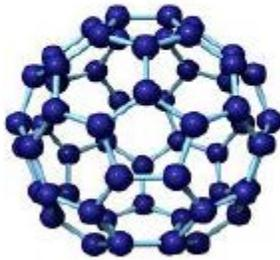
*diamond*



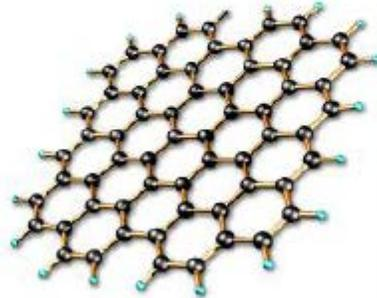
*lonsdaleite*



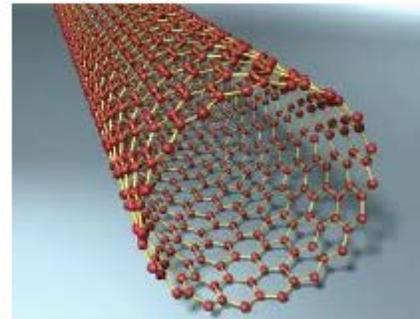
*graphite*



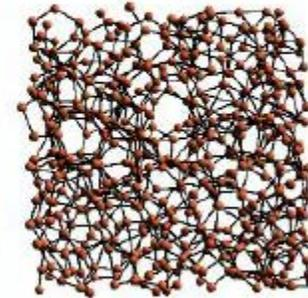
*fullerene*



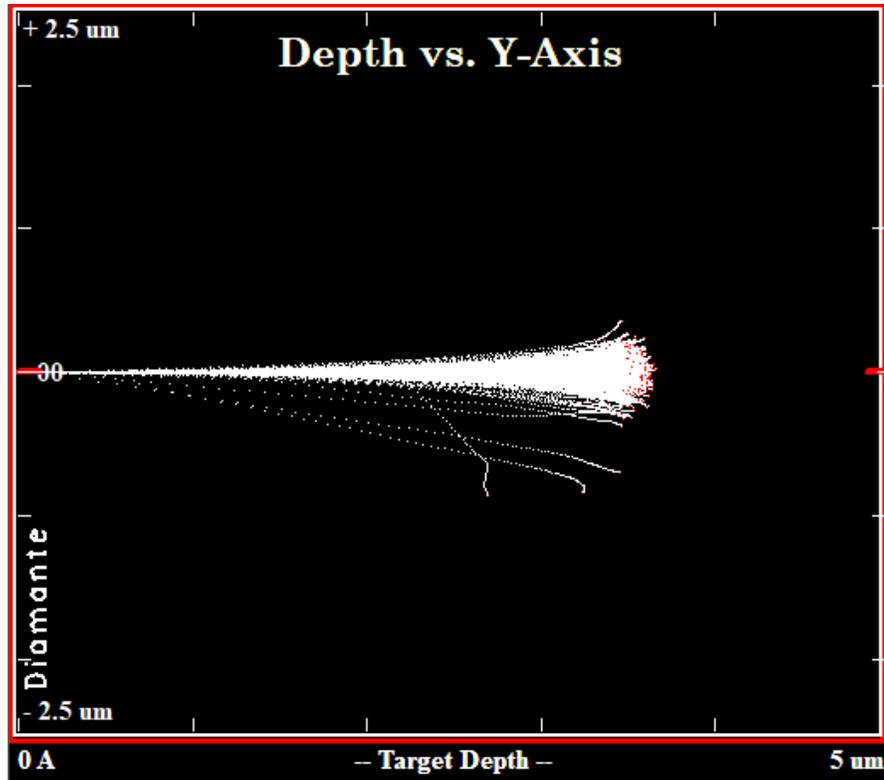
*graphene*



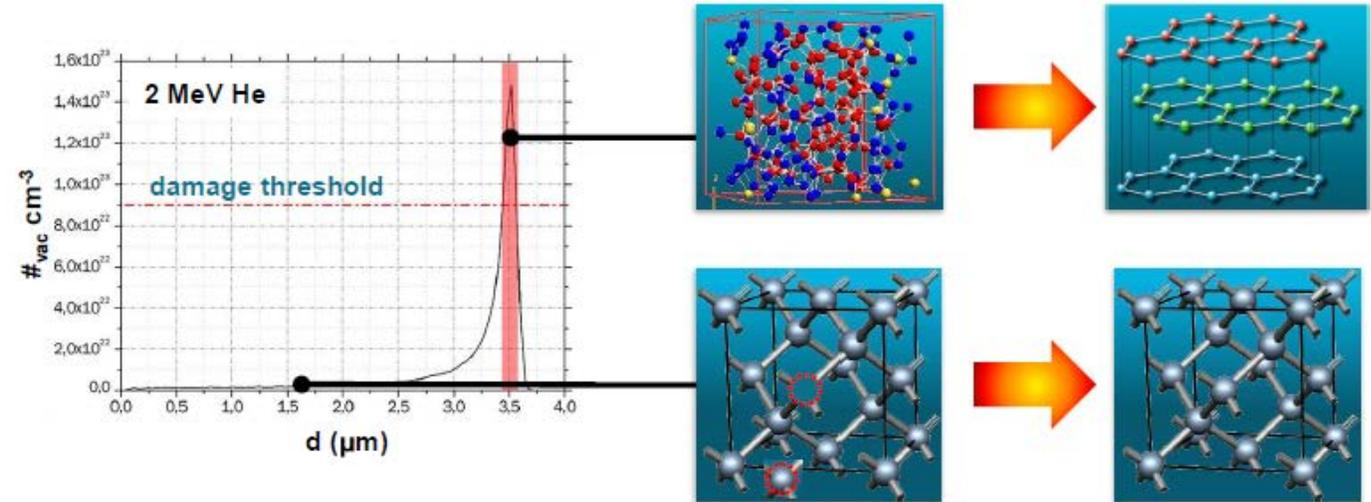
*nanotube*



*amorphous carbon*



### Thermal annealing



- **Above** threshold: amorphous carbon → polycrystalline graphite
- **Below** threshold: diamond with Frenkel defects → diamond

# The diamond lift-off technique

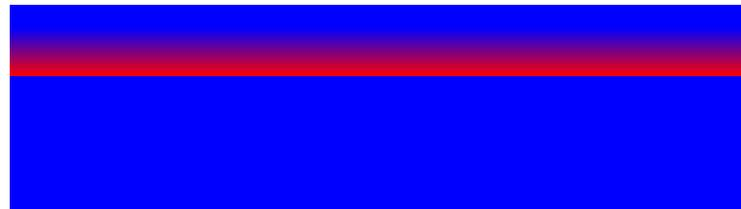
## Single-crystal diamond plate liftoff achieved by ion implantation and subsequent annealing

N. R. Parikh, J. D. Hunn, E. McGucken, and M. L. Swanson  
*University of North Carolina, Chapel Hill, North Carolina 27599-3255*

C. W. White  
*Oak Ridge National Laboratory, Oak Ridge, Tennessee 37831-6048*

R. A. Rudder, D. P. Malta, J. B. Posthill, and R. J. Markunas  
*Research Triangle Institute, Research Triangle Park, North Carolina 27709-2194*

Appl. Phys. Lett. **61** (26), 28 December 1992 3124



- **MeV ion implantation**

# The diamond lift-off technique

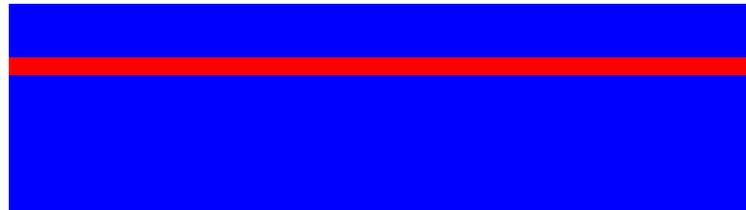
## Single-crystal diamond plate liftoff achieved by ion implantation and subsequent annealing

N. R. Parikh, J. D. Hunn, E. McGucken, and M. L. Swanson  
*University of North Carolina, Chapel Hill, North Carolina 27599-3235*

C. W. White  
*Oak Ridge National Laboratory, Oak Ridge, Tennessee 37831-6048*

R. A. Rudder, D. P. Malta, J. B. Posthill, and R. J. Markunas  
*Research Triangle Institute, Research Triangle Park, North Carolina 27709-2194*

*Appl. Phys. Lett.* **61** (26), 28 December 1992 3124



- **MeV ion implantation**
- **Thermal annealing**

# The diamond lift-off technique

## Single-crystal diamond plate liftoff achieved by ion implantation and subsequent annealing

N. R. Parikh, J. D. Hunn, E. McGucken, and M. L. Swanson  
*University of North Carolina, Chapel Hill, North Carolina 27599-3255*

C. W. White  
*Oak Ridge National Laboratory, Oak Ridge, Tennessee 37831-6048*

R. A. Rudder, D. P. Malta, J. B. Posthill, and R. J. Markunas  
*Research Triangle Institute, Research Triangle Park, North Carolina 27709-2194*

Appl. Phys. Lett. **61** (26), 28 December 1992 3124



- **MeV ion implantation**
- **Thermal annealing**
- **Selective graphite etching**

# The diamond lift-off technique

## Single-crystal diamond plate liftoff achieved by ion implantation and subsequent annealing

N. R. Parikh, J. D. Hunn, E. McGucken, and M. L. Swanson  
*University of North Carolina, Chapel Hill, North Carolina 27599-3255*

C. W. White  
*Oak Ridge National Laboratory, Oak Ridge, Tennessee 37831-6048*

R. A. Rudder, D. P. Malta, J. B. Posthill, and R. J. Markunas  
*Research Triangle Institute, Research Triangle Park, North Carolina 27709-2194*

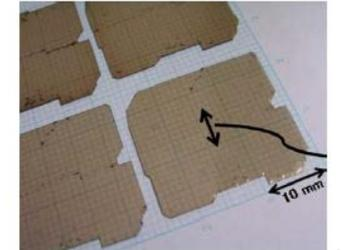
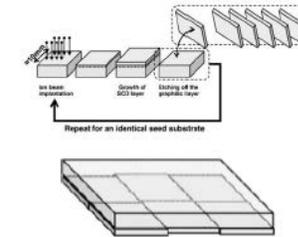
Appl. Phys. Lett. **61** (26), 26 December 1992 3124

Lift-off + CVD growth



Developments of elemental technologies to produce inch-size single-crystal diamond wafers<sup>1,2</sup>

Hideaki Yamada<sup>1</sup>, Akiyoshi Chayahara, Yoshiaki Makino, Nobuteru Tsubouchi, Shin-ichi Shikata, Naoki Fujimori<sup>1</sup>



- MeV ion implantation
- Thermal annealing
- Selective graphite etching
- Lift-out

# Lift-off + laser micro-cutting

## Fabrication of single-crystal diamond microcomponents

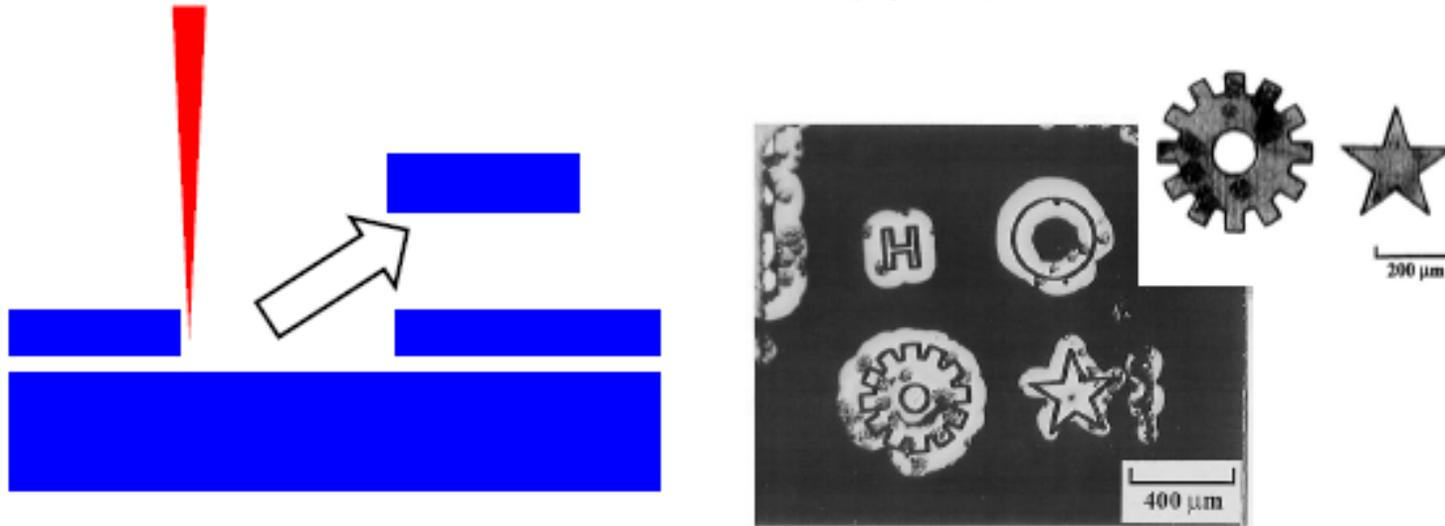
John D. Hunn, S. P. Withrow, C. W. White, R. E. Clausing, and L. Heatherly  
*Oak Ridge National Laboratory, Bldg. 5500 MS-6376, Oak Ridge, Tennessee 37831-6276*

C. Paul Christensen  
*Potomac Photonics, Lanham, Maryland 20703*

(Received 26 August 1994; accepted for publication 7 October 1994)

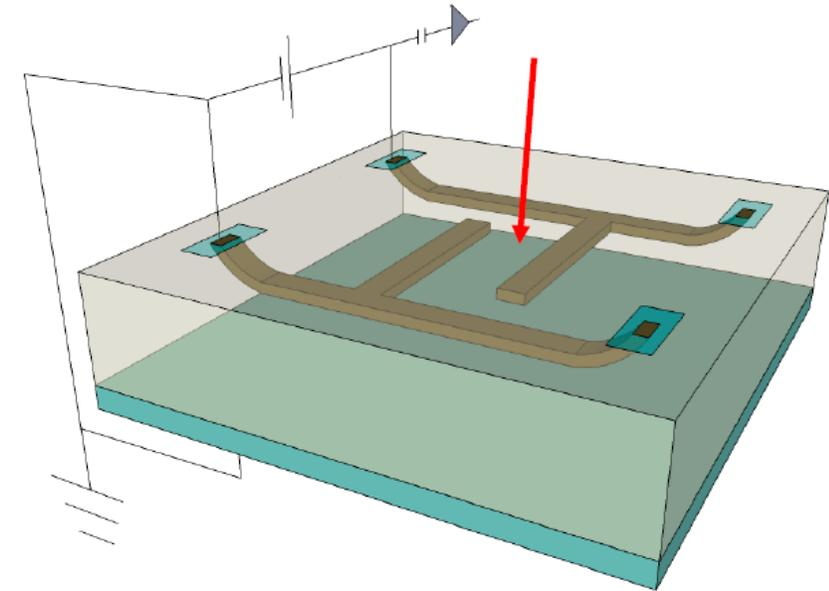
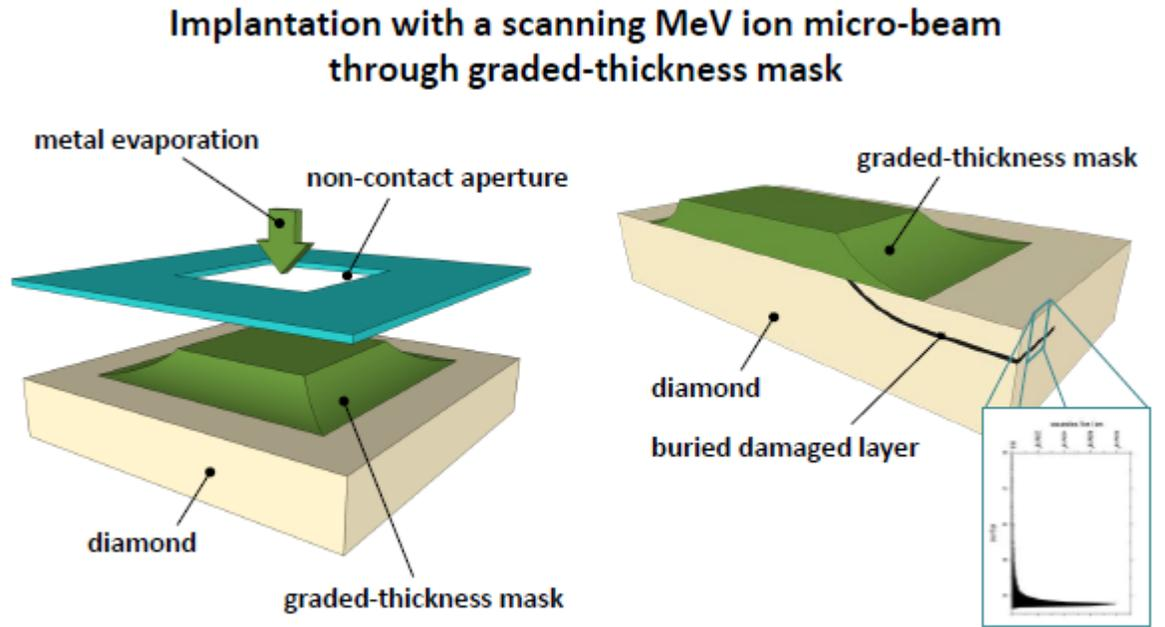
We have combined a technique for the lift-off of thin diamond films from a bulk diamond with a technique for engraving diamond with a focused excimer laser to produce free-standing single-crystal diamond microstructures. One microcomponent that has been produced is a 12 tooth gear  $\sim 400 \mu\text{m}$  in diameter and  $\sim 13 \mu\text{m}$  thick. Other microstructures have also been demonstrated, showing the versatility of this method. This process should be applicable to producing diamond microcomponents down to spatial dimensions (width and thickness) of a few micrometers. © 1994 American Institute of Physics.

3072 Appl. Phys. Lett. 65 (25), 12 December 1994



# MICRO CONTATTI

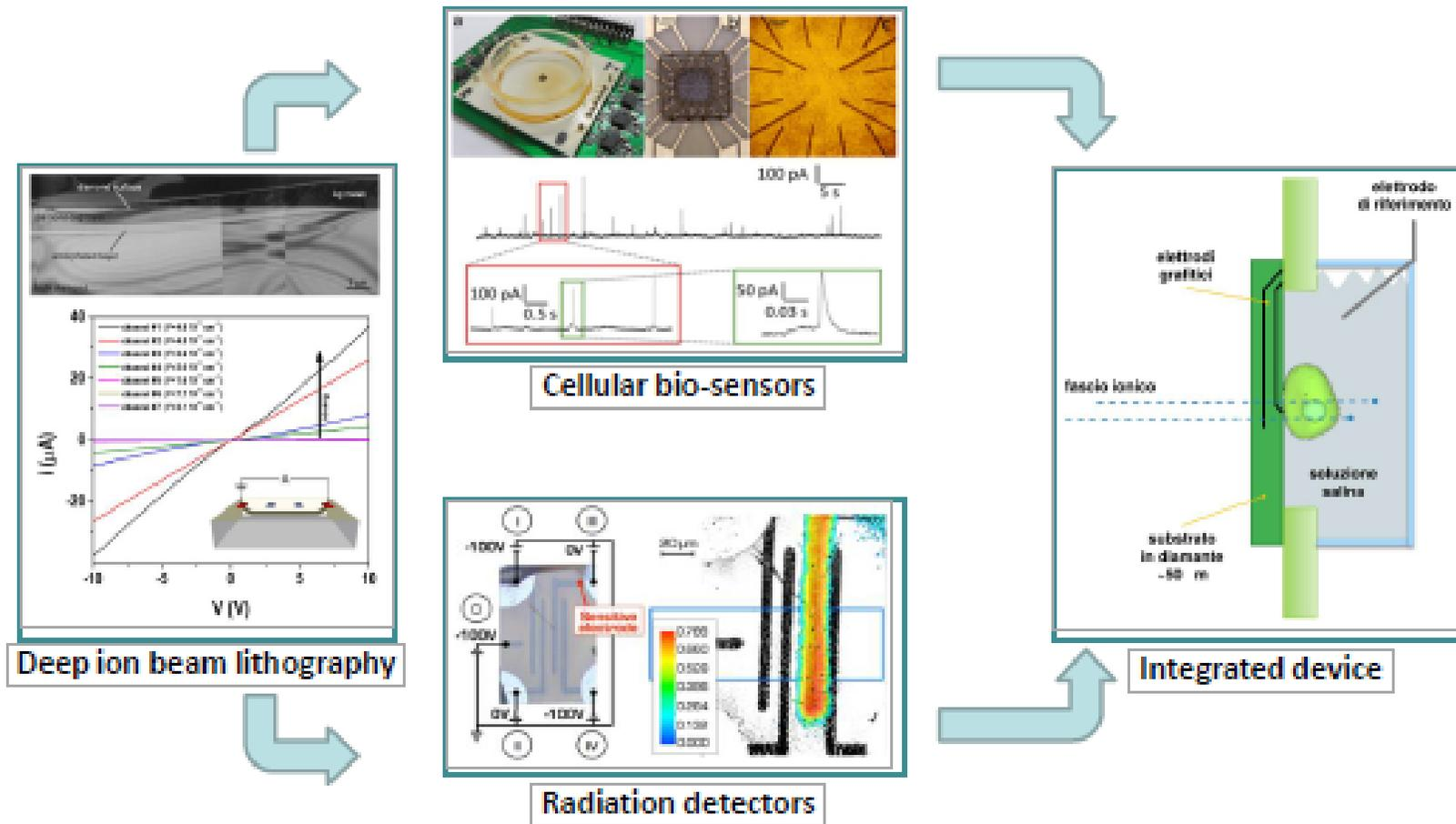
- RIVELATORI DI RADIAZIONE SENSIBILI ALLA POSIZIONE
- MICRO-SENSORI BIOLOGICI



→ direct writing of **sub-superficial conductive microchannels** in single-crystal diamond

# SENSORI E RIVELATORI A DIAMANTE

Development of artificial diamond devices for the simultaneous detection of cell signals and ionizing radiation for applications in micro-radiobiology



# DIAMANTE AMORFO ?

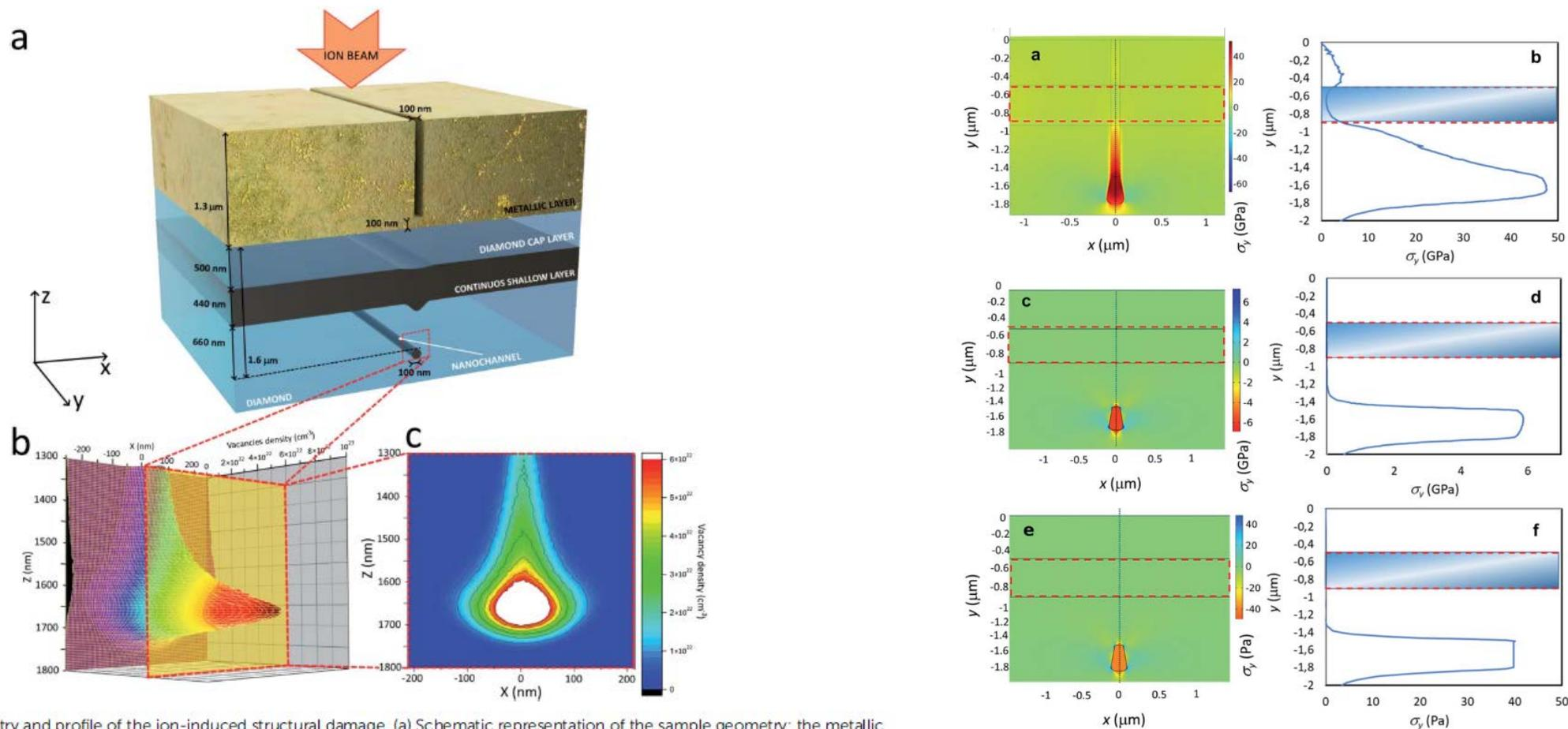
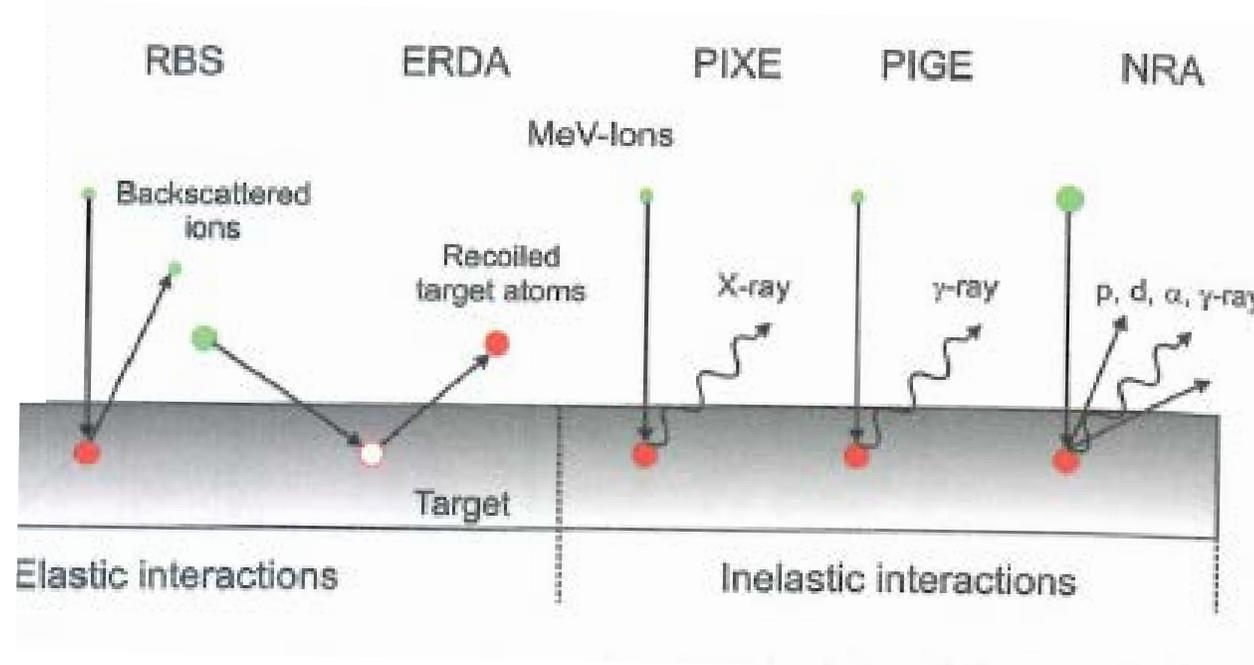
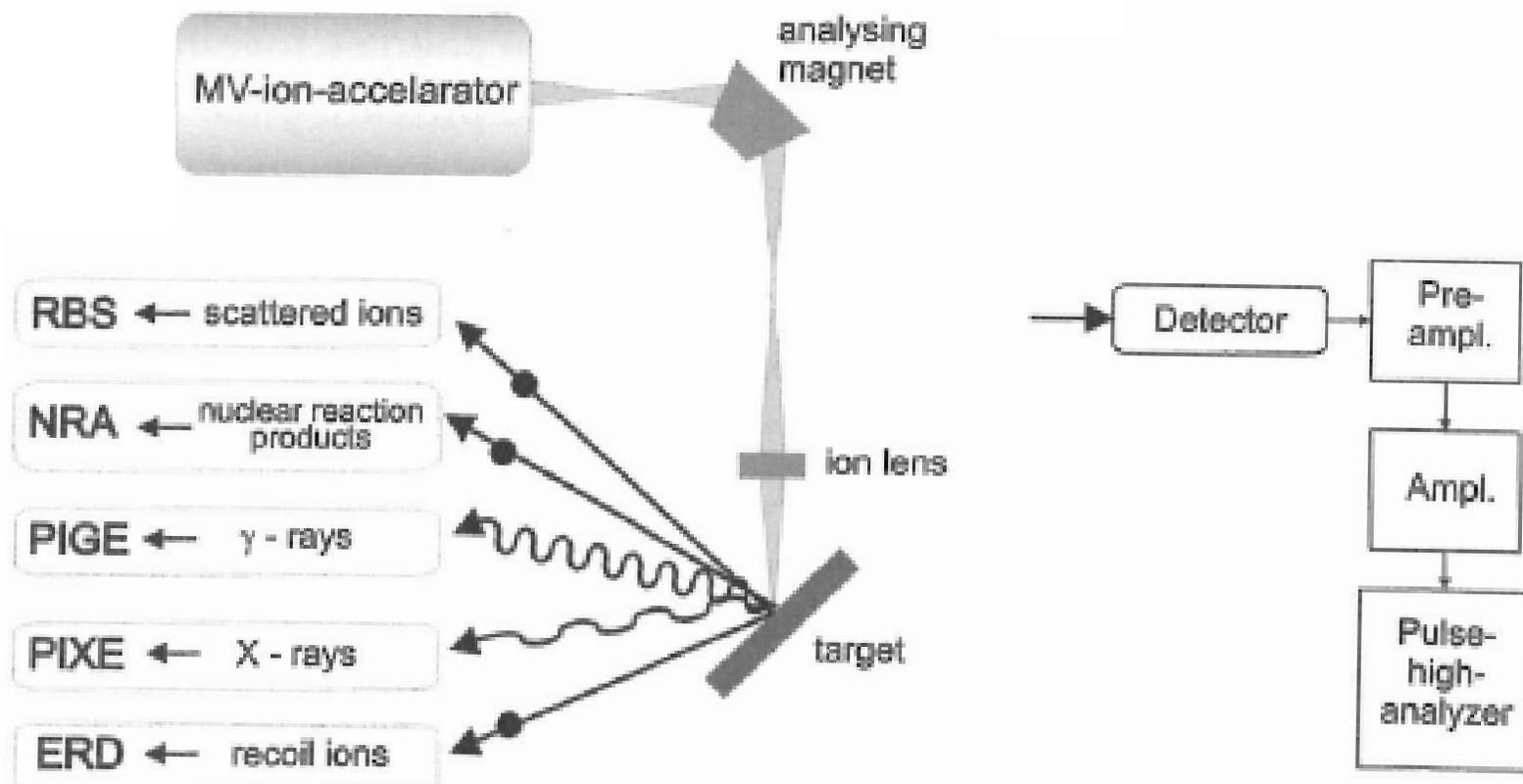


Fig. 1 Sample geometry and profile of the ion-induced structural damage. (a) Schematic representation of the sample geometry: the metallic mask with the nanometric aperture determines the formation of both the continuous shallow layer and of the nanochannel upon MeV ion irradiation. (b) Three-dimensional plot of the cross-sectional profile of ion-induced damage density as resulting from SRIM simulation. (c) Corresponding two-dimensional plot: the size and shape of the region damaged beyond the estimated critical threshold (in red) corresponds to the features observed in Fig. 4a; note that the same plot is reported as an inset of Fig. 4a for sake of comparison with experimental data.

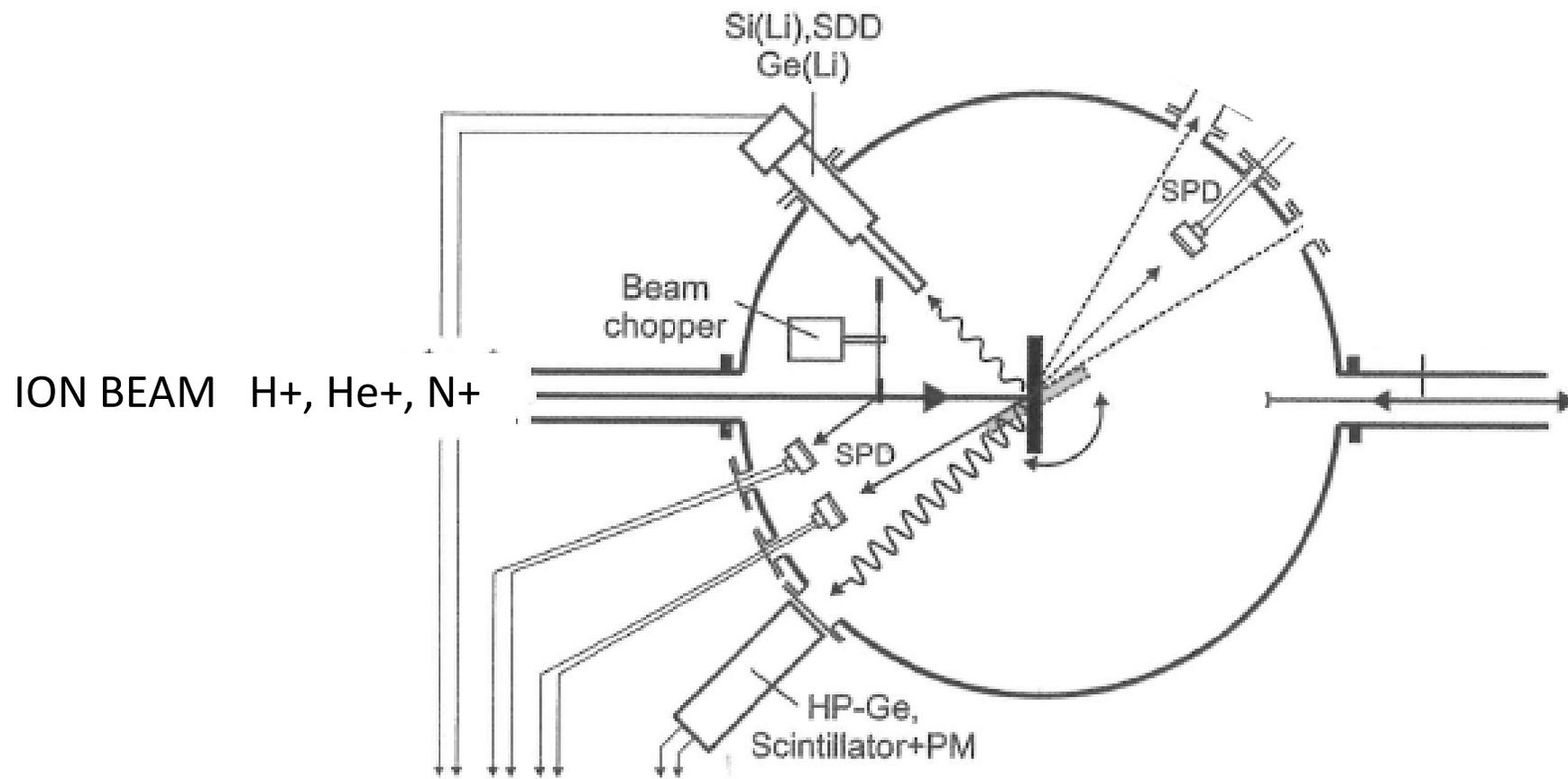
Nanoscale Advances, 2021, DOI: 10.1039/D1NA00136A

# ACCELERATORI DI IONI PER ANALISI DEI MATERIALI





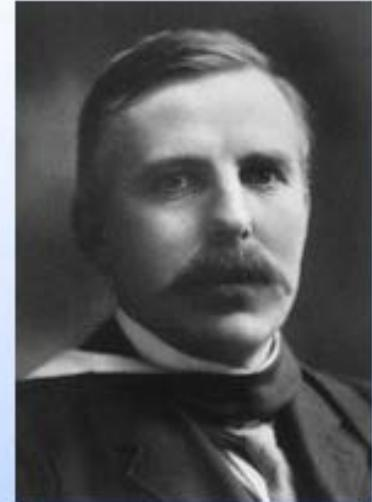
Schematic overview of accelerator-based IBA techniques (a) and radiation detection system arrangement (b) for particle and photon radiations emitted from a target surface during ion–solid interaction



Experimental setup for combined IBA techniques (schematically, after [9, 10])

## Sir Ernest Rutherford (1871 - 1937)

- 1911: Rutherford's scattering experiments:  $^4\text{He}$  on Au  
⇒ Atomic nucleus, nature of the atom



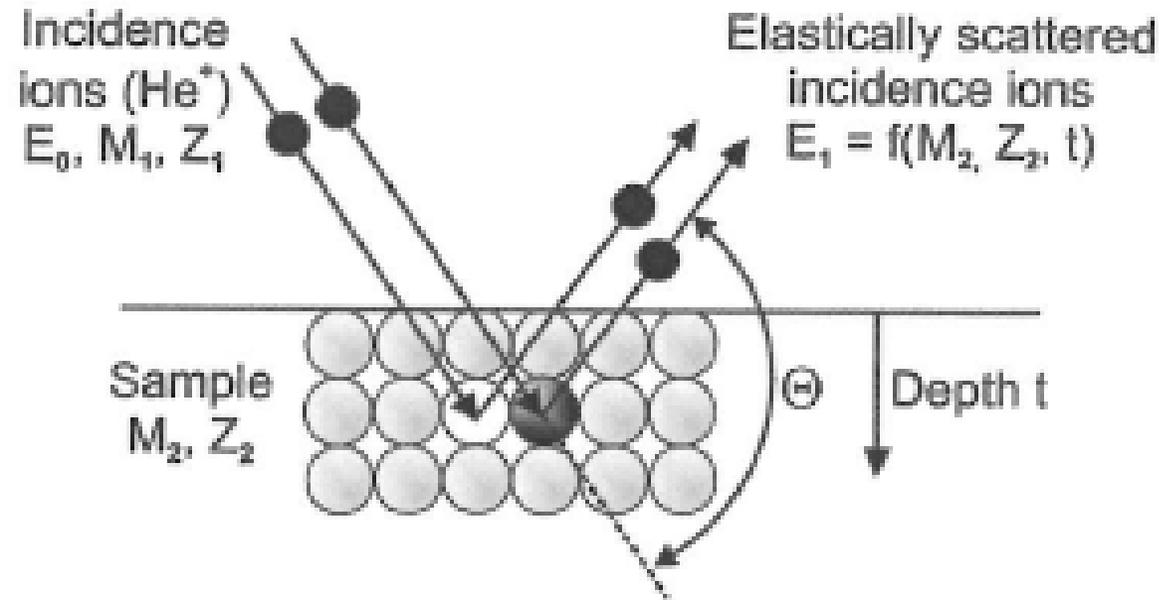
## RBS as materials analysis method

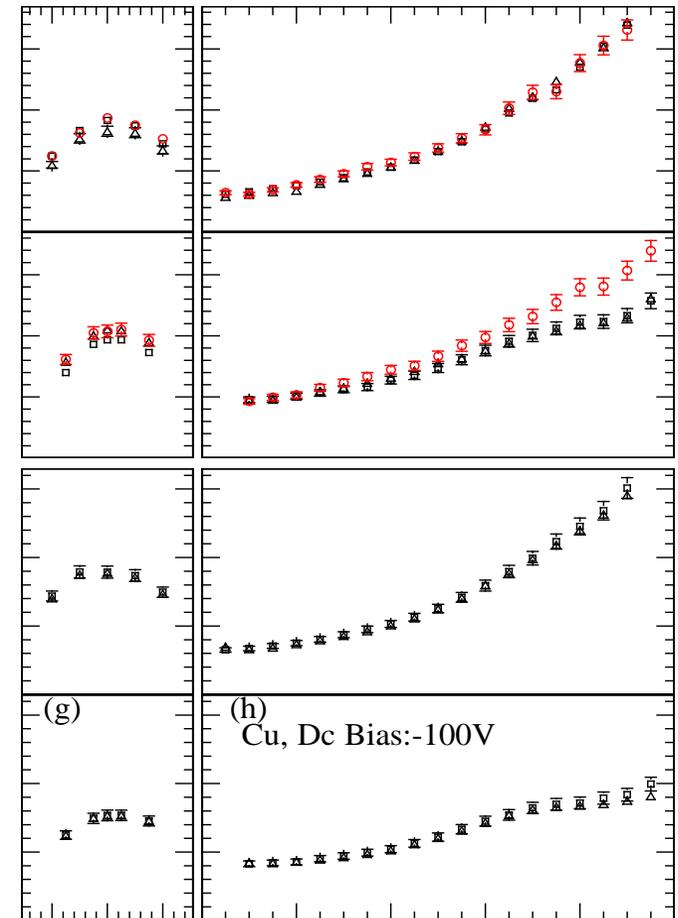
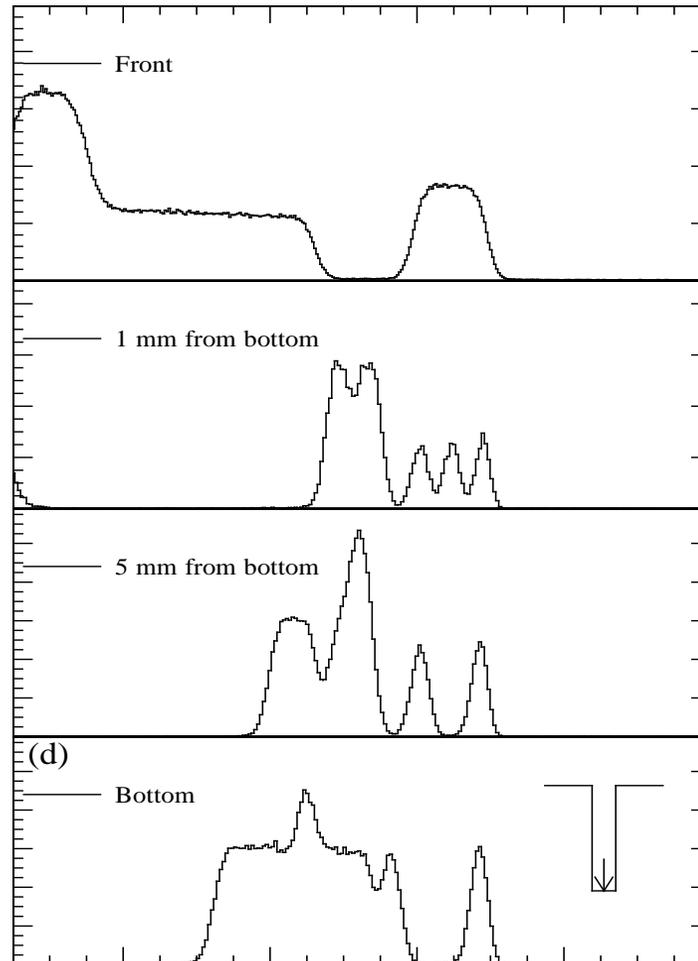
- 1957: S. Rubin, T.O. Passell, E. Bailey, "Chemical Analysis of Surfaces by Nuclear Methods", *Analytical Chemistry* 29 (1957) 736

"Nuclear scattering and nuclear reactions induced by high energy protons and deuterons have been applied to the analysis of solid surfaces. The theory of the scattering method, and determination of O, Al, Si, S, Ca, Fe, Cu, Ag, Ba, and Pb by scattering method are described. C, N, O, F, and Na were also determined by nuclear reactions other than scattering. The methods are applicable to the detection of all elements to a depth of several  $\mu\text{m}$ , with sensitivities in the range of  $10^{-8}$  to  $10^{-6}$  g/cm<sup>2</sup>."

# RBS

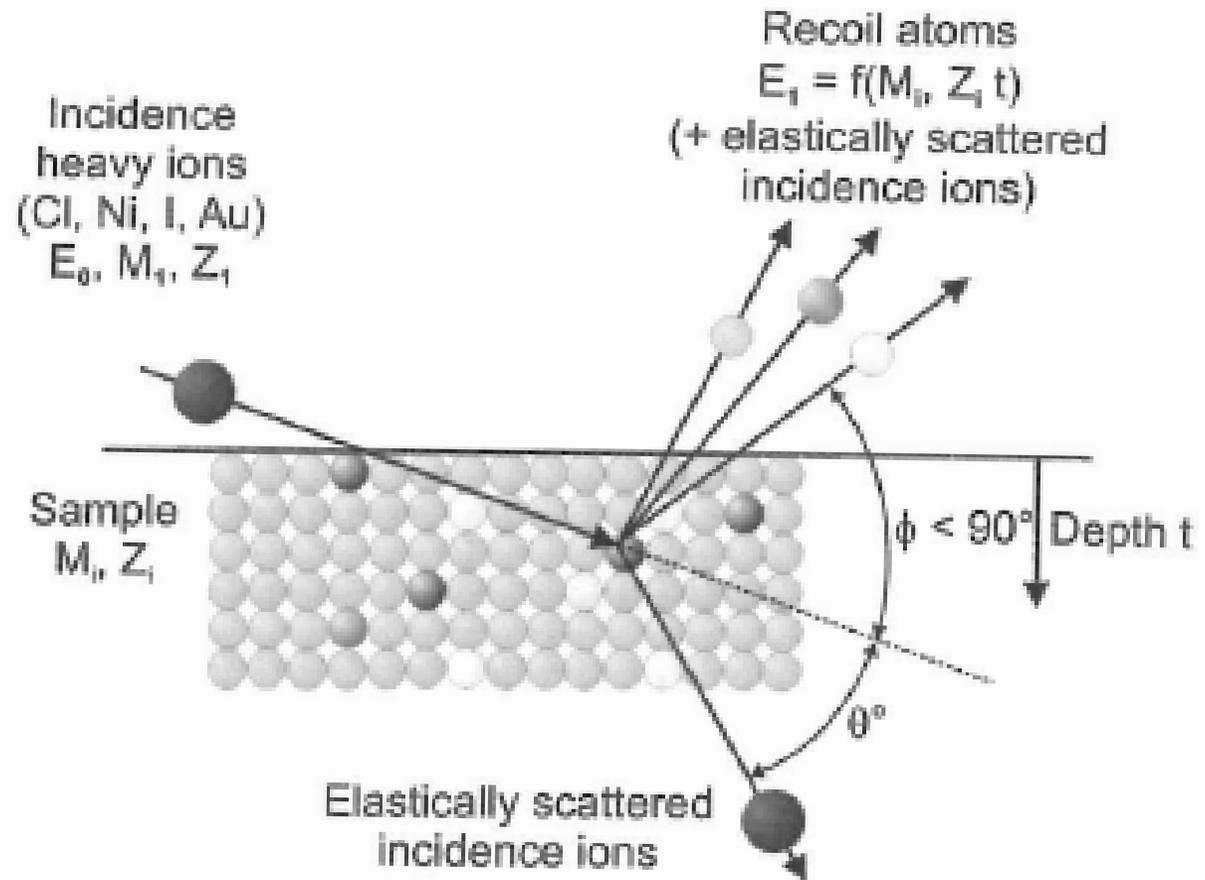
Physical principle  
of Rutherford backscattering  
(schematically)



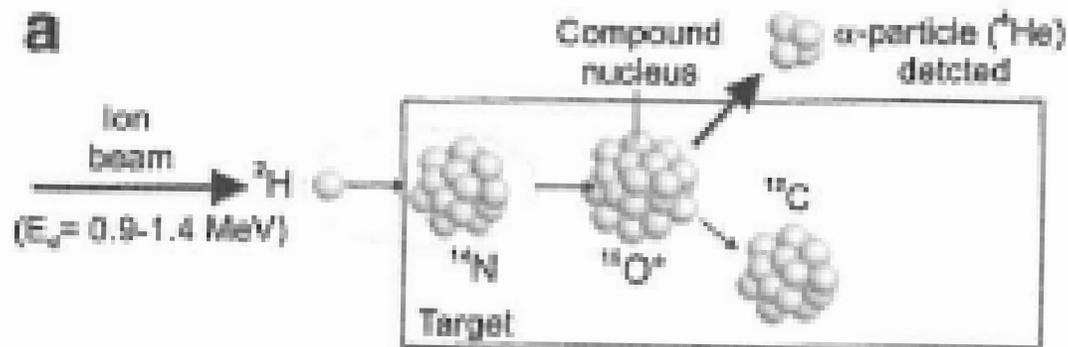


# ERD

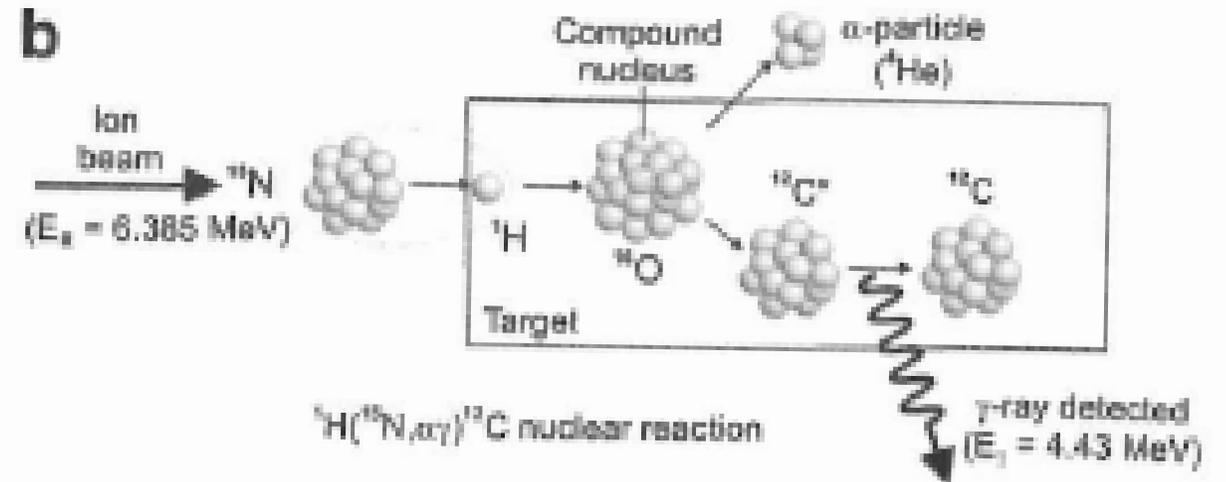
Physical principle of elastic recoil detection analysis (ERDA) with  $\theta$  the scattering angle and  $\phi$  the recoil angle which is actually the detector angle



# NRA



$^{14}\text{N}(d,\alpha)^{12}\text{C}$  nuclear reaction

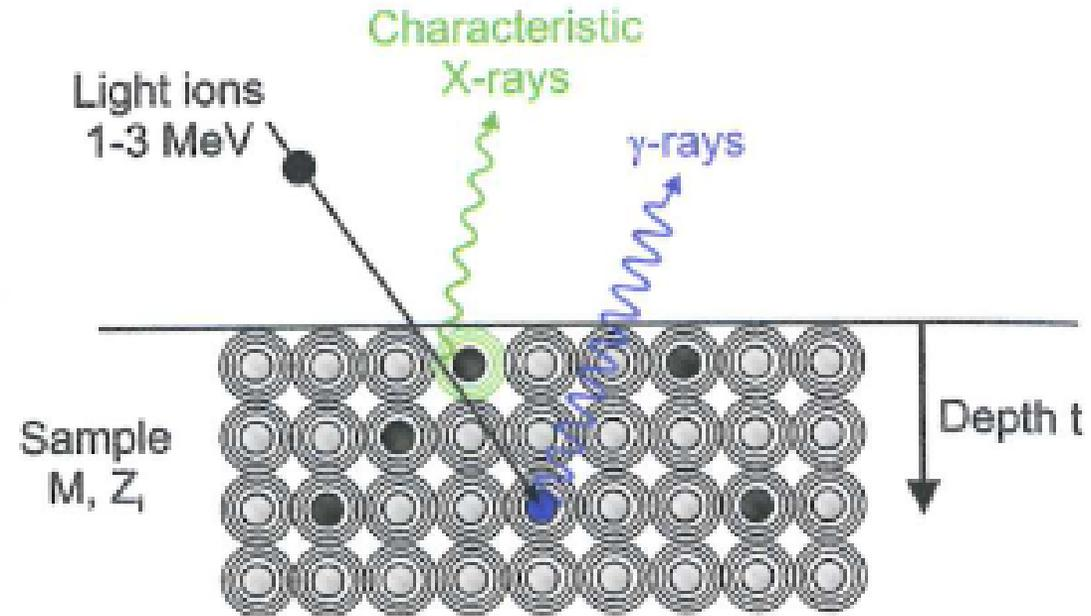


$^1\text{H}(^{15}\text{N},\alpha\gamma)^{12}\text{C}$  nuclear reaction

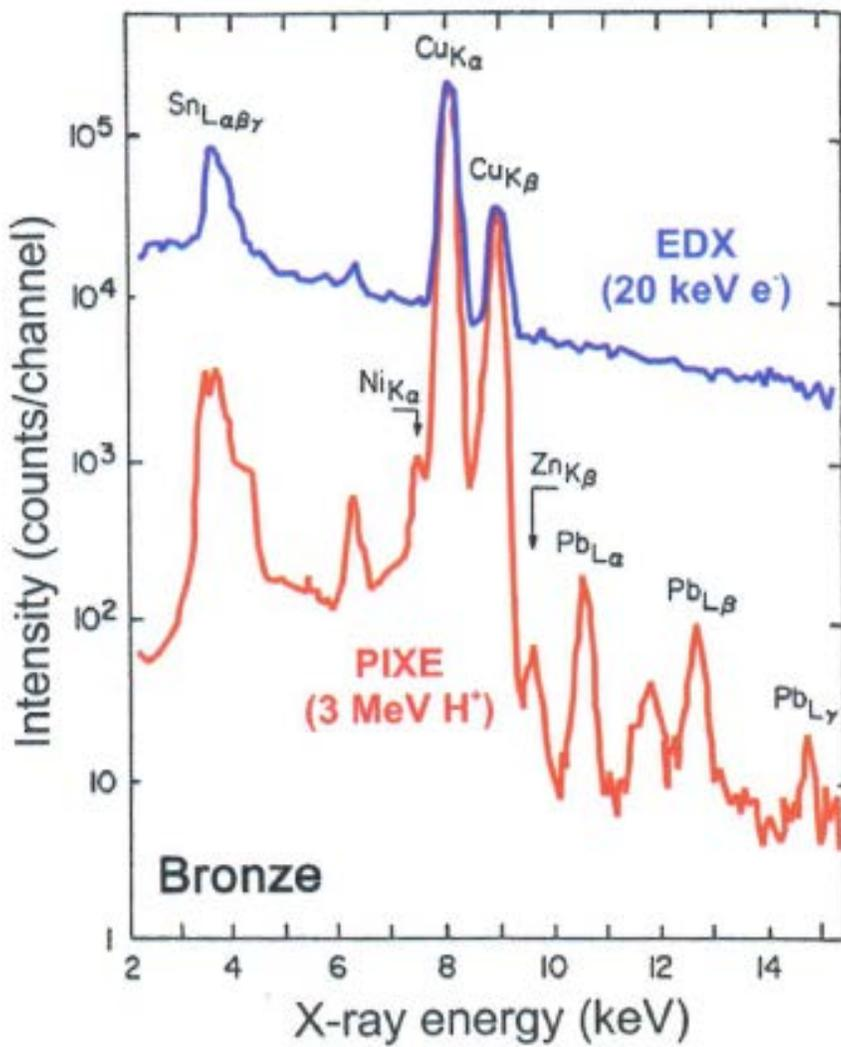
Physical principle of nuclear reaction analysis (NRA) for two typical reactions: (a)  $^{14}\text{N}(d,\alpha)^{12}\text{C}$  nuclear reaction with detection of the emitted  $\alpha$ -particle for depth profiling of nitrogen, and (b)  $^1\text{H}(^{15}\text{N},\alpha\gamma)^{12}\text{C}$  nuclear reaction with the detection of the emitted  $\gamma$ -ray for depth profiling of hydrogen

# PIXE, PIGE

Physical scheme  
of ion induced photon  
emission from atomic  
electron shells (X-ray)  
or atomic nuclei ( $\gamma$ -ray)



Comparison of PIXE (red line) and EDX (blue line) spectra taken from a bronze sample. PIXE is generally about 100 times more element sensitive [4]





E QUESTO E' SOLO UN ASSAGGIO DELLE  
POTENZIALITA' OFFERTE DALL'IMPIEGO DI IONI  
ACCELERATI NELLA SCIENZA E TECNOLOGIA

Grazie per l'attenzione